1962

Dynamic response characteristics of fluid transmission lines

Bruce Leland Johnson
Iowa State University

DYNAMIC RESPONSE CHARACTERISTICS OF FLUID TRANSMISSION LINES

by

Bruce Leland Johnson

A Dissertation Submitted to the
Graduate Faculty in Partial Fulfillment of
The Requirements for the Degree of
DOCTOR OF PHILOSOPHY

Major Subjects: Mechanical Engineering
Electrical Engineering

Approved:

Signature was redacted for privacy.

In Charge of Major Work

Signature was redacted for privacy.

Heads of Major Departments

Signature was redacted for privacy.

Dean of Graduate College

Iowa State University
Of Science and Technology
Ames, Iowa

1962

TABLE OF CONTENTS

INTRODUCTION

Recent emphasis on control theory and system stability has made the dynamic output-input relationship of system components a prime factor in overall system synthesis, and the study of dynamic response characteristics has occupied the attention of many investigators. Because in fluid systems it is necessary to transport the working fluid from one major component to another through conduits or pipes, and because the dynamics of these pipe lines may contribute a great deal to a tendency toward system instability, the dynamic response characteristics of these lines are of interest to designers.

When the load impedance (e.g., valve resistance) at the output of a fluid transmission line is varied, transient pressures appear at the load. The dynamic phenomena associated with the changing load impedance have historically been termed water hammer. Investigations in this area have been primarily concerned with the peak pressure that would occur in a piping system when the flow of a compressible fluid in an elastic pipe was stopped or restricted in a given manner.

In the analysis and synthesis of these systems the simulation on an analog computer of the complete system including the transmission lines has been of great value. Unfortunately, present mathematical models of the prototype pipe have not been formulated in such a way as to lend themselves conveni-

ently, efficiently and/or accurately to simulation on an analog computer.

The present investigation was begun to formulate the mathematical model of a fluid transmission line in such a way that the dynamic response characteristics of such a line would be apparent and readily simulated on an analog computer. One such formulation might be the so called transfer function, which is the ratio of the Laplace transform of the output pressure to the Laplace transform of the input pressure. Experimental verification of the mathematical model was considered to be necessary. The verification procedure consisted of pressure pulsing a liquid-filled pipe at one end and comparing the transfer function computed from the output- and input-pressure waveforms to the transfer function of the formulated mathematical model.

The work reported herein was performed during the years 1960 to 1962 in the Mechanical Engineering Department, Iowa State University, Ames, Iowa.

HISTORICAL BACKGROUND OF FLUID TRANSMISSION LINE THEORY AND EXPERIMENT

Development of the Theory Relating to Water Hammer

At the turn of the twentieth century the Russian physicist, Nicolai Egorovich Joukovsky, and the Italian engineer, Lorenzo Allievi, working independently, demonstrated that the dynamic phenomenon known as water hammer was an acoustic wave action and could be described mathematically by the classical wave equation (1),

$$\frac{\partial^2 H}{\partial t^2} = a^2 \frac{\partial^2 H}{\partial x^2} .$$

It was then possible to apply the existing results of many investigators, including those of the mathematicians d'Alembert, Euler, Daniel Bernoulli, Fourier, Poisson and Liouville, who had solved the wave equation by various methods in the late 1700's and early 1800's. Also, in 1848 Wertheim had discovered that the actual velocity of sound through water contained in pipes was less than the theoretical value based only on the compressibility of the water. In that same year Helmholtz correctly ascribed this fact to the elasticity of the pipe walls. In 1878 Korteweg combined the effects of elasticity of both the fluid and the pipe and gave the first accurate formula for the velocity of sound in a thin-walled pipe.

In the years following the original works of Joukovsky

and Allievi, the phenomenon of water hammer, which occurs when the flow of a fluid through a pipe is interrupted, was the subject of exhaustive theoretical and experimental investigation. The vast majority of solutions to water hammer problems involved graphical procedures, or were mathematical solutions to problems involving very special types of flow interruptions.

General Response Characteristics of Hydraulic Lines

After World War II, during which many advances were made in the field of automatic control and feedback theory, interest in the dynamic response of fluid transmission lines was revived in a new light.

In 1953 Lee et al. (2) included the effect of the fuel lines in their investigations into the stability and control of liquid-propellant rocket systems. In the next few years much work was done on the low-frequency combustion instability phenomenon called "chugging" that appeared in these systems. In 1954 Sabersky (3) attributed a part of the cause of this instability to the dynamic characteristics of the fuel-feed lines.

In 1956 Chang (4) noted the significant dynamic effect that supply conduits had on hydraulic control systems, specifically on the stability of control valves.

In the intervening years efforts have been made to better

represent the fluid line mathematically for greater ease of simulation and synthesis of systems. There has, however, been little or no published experimental verification to date.

Simulation of Hydraulic System Components

The concept of analog simulation to effect a rapid analysis or an efficient synthesis of various systems has been understood and applied for many years (5). As an example, in 1952 Paynter (6) suggested some electrical analogies and analog computer programs for hydraulic analysis. Since that time, many investigators have used the analog computer as a tool in the analysis of their hydraulic control problems using various simulation or programming methods to represent the dynamic response characteristics of a fluid transmission line (7, 8).

RESEARCH RELATED TO DYNAMIC RESPONSE CHARACTERISTICS OF FLUID TRANSMISSION LINES

The discovery by Joukovsky and Allievi that the dynamic pressure disturbance which occurred in a pipeline when the flow was stopped or suddenly restricted was an acoustic wave action allowed investigators studying water hammer to apply the existing knowledge of the velocity of sound in water confined in a pipe and the solutions to the wave equation to the problem. Joukovsky carried out extensive experiments with pipes of two, four, six and twenty-four inch diameters, and lengths over one thousand feet. His investigation included the study of the effects of air chambers, leaks and rate of gate (valve) closure on the transient pressure (9).

Following Joukovsky and Allievi, a great deal of experimentation was done, and graphical methods for analyzing water hammer problems were proposed and refined (1, 10, 11, 12, 13, 14).

Until 1945, the analysis of water hammer was done graphically for all but very special cases of valve closure. At this time, Rich (15) presented a method for analyzing water hammer by the use of the Laplace-Mellin transformation. Again, as with other mathematical solutions, only a few special cases of valve closure could be handled with this method.

The effect of friction poses a formidable problem because

of its non-linear characteristics. Several investigators have treated friction as linear and showed that, for such an assumption, previous results to water hammer problems which assumed no friction would be modified by an exponential (15, 16, 17, 18). This analysis proved to match experimental results more closely. Helmholtz and Kirchhoff developed a theory for the damping of small amplitude vibrations of a fluid in a cylindrical tube with the assumptions of laminar flow and sinusoidal pressure waves. Binder modified this by the addition of an eddy viscosity term to take into account inertia forces (19, p. 312; 20). Based on this analysis, the effect of friction becomes a function of velocity to the three halves power, which would mean that higher frequency waves would be attenuated more than the linear assumption indicates. Brown (21) came to the same conclusion about the higher frequency waves when he took into account the effect of variable resistance due to the changing velocity profile and the effect of variable fluid capacitance due to heat transfer.

Some of the earlier work in rocket fuel system stability analysis assumed the fuel feed lines as inelastic and the fuel as incompressible (2). When it was realized that the dynamics of the fuel line played an appreciable part in the system's stability characteristics (3) other investigators made an attempt to include these characteristics in the system analysis.

Their analyses represented the line as a lumped parameter system, dividing the line into lumped constants with a length up to one fourth the minimum wave length of interest in the analysis (7, 22). The effect of friction was taken into account by some investigators by lumping the resistance at either end of the pipe (friction joints) (23, 24).

Li's (25) analysis of the dynamic characteristics of a fuel line took two forms. First, with the assumption of an incompressible fuel supply system, considering the effect of acceleration only, he arrived at a first order system for the mathematical model. He also showed, when considering the actual compressibility of the system, that as the load resistance was increased the line would again have dynamic characteristics approaching those of a first order system.

Regetz (26) determined experimentally, for sinusoidal inputs, the input impedance for a stainless-steel line one inch in diameter and sixty-eight feet in length. With a resistance as the load impedance and input frequencies from 0.5 to 90 c.p.s. he determined that the input impedance would vary approximately sinusoidally as a function of input frequency (as was deduced by Lee et al. (27)). The significant effect of pipe vibration indicated that the method of pipe support was an important consideration. For the frequencies studied the effect of friction was negligible. As the load impedance

approached the characteristic impedance of the pipe the input impedance approached a constant function of frequency. In other words, if the line were terminated with an impedance equal to the line's characteristic impedance the reflected wave would disappear.

This last fact was shown by Chang (4) to be a method for matching the supply line to a control valve in a hydraulic system for stability. Ezekiel (28) also studied the effect of supply line dynamics on control valve stability.

Skalak (29) has shown that for sharp wave fronts a small disturbance due to the pipe vibration will travel down the pipe faster than the main wave and thus create a transient pressure not predicted by earlier theory. These waves are called precursor waves.

ANALYSIS OF THE TRANSMISSION LINE PROBLEM

This section presents the analytical procedures and assumptions used to arrive at the transfer function of a hydraulic transmission line. Reference is made to the section entitled SYMBOLS AND NOTATION, in which the terminology is defined, and the section entitled DERIVATION OF ONE-DIMENSIONAL DYNAMIC EQUATIONS.

The transfer function is defined for purposes of this investigation as the ratio of the Laplace transform of the pressure at the load end of the line to the Laplace transform of the pressure at the input to the line with zero initial conditions,

$$\overline{W}(s) = \frac{\overline{H}(L,s)}{\overline{H}(0,s)} . \tag{1}$$

The terms "pressure" and "velocity" refer to the perturbation values, that is, the difference between the actual values and the steady-state values;

$$H(x,t) = \mathcal{H}(x,t) - H_o(x), \tag{2}$$

and

$$V(x,t) = \mathcal{V}(x,t) - V_o(x). \tag{3}$$

Load impedance is defined as the ratio of the Laplace transform of the pressure to the Laplace transform of the velocity, both taken at the load end,

$$Z_L = \frac{\overline{H}(L,s)}{\overline{V}(L,s)} . \tag{4}$$

The dynamic equations relating velocity and pressure are

$$-\frac{H(x,t)}{x} = \frac{1}{g}\frac{V(x,t)}{t} + FV(x,t) \tag{5}$$

$$-\frac{V(x,t)}{x} = \frac{g}{a^2}\frac{H(x,t)}{t} \tag{6}$$

The initial conditions are

$$H(x,0) = 0 \quad \text{and} \quad V(x,0) = 0. \tag{7}$$

After taking the Laplace transform with respect to the time variable t, equations 5 and 6 become

$$-\frac{d\bar{H}(x,s)}{dx} = \frac{1}{g}[s\bar{V}(x,s) - V(x,0)] + F\bar{V}(x,s) \tag{8}$$

and

$$-\frac{d\bar{V}(x,s)}{dx} = \frac{g}{a^2}[s\bar{H}(x,s) - H(x,0)]\,. \tag{9}$$

Referring to equations 7 and letting the arguments of the transformed pressure and velocity be understood, equations 8 and 9 become

$$-\frac{d\bar{H}}{dx} = \left(\frac{s}{g} + F\right)\bar{V} \tag{10}$$

and

$$-\frac{d\bar{V}}{dx} = \frac{gs\bar{H}}{a^2}\,. \tag{11}$$

From equation 10

$$-\frac{d^2\bar{H}}{dx^2} = \left(\frac{s}{g} + F\right)\frac{d\bar{V}}{dx}\,, \tag{12}$$

and substituting into this equation 11

$$\frac{d^2\bar{H}}{dx^2} = \frac{gs}{a^2}\left(\frac{s}{g} + F\right)\bar{H}\,. \tag{13}$$

Letting

$$n^2 = \frac{gs}{a^2}\left(\frac{s}{g} + F\right) \tag{14}$$

equation 13 becomes

$$\frac{d^2\overline{H}}{dx^2} - n^2\overline{H} = 0 \ , \tag{15}$$

and by a similar series of steps

$$\frac{d^2\overline{V}}{dx^2} - n^2\overline{V} = 0 \ . \tag{16}$$

The solutions to equations 15 and 16 are of the form

$$\overline{H} = Ae^{-nx} + Be^{nx} \tag{17}$$

and

$$\overline{V} = Ce^{-nx} + De^{nx} \ , \tag{18}$$

and therefore from equations 11 and 18

$$-\frac{d\overline{V}}{dx} = Cne^{-nx} - Dne^{nx} = \frac{gs}{a^2}(Ae^{-nx} + Be^{nx}). \tag{19}$$

Letting

$$Z_o = \frac{na^2}{gs} = \frac{a}{g}\sqrt{\frac{1+Fg}{s}} \tag{20}$$

it was found when equating like coefficients that

$$C = \frac{A}{Z_o} \quad \text{and} \quad D = \frac{-B}{Z_o} \ , \tag{21}$$

and then from equation 18

$$\overline{V} = \frac{Ae^{-nx}}{Z_o} - \frac{Be^{nx}}{Z_o} \ . \tag{22}$$

Evaluating both $\overline{V}$ and $\overline{H}$ at $x = L$

$$\frac{\overline{H}(L,s)}{Z_o\overline{V}(L,s)} = \frac{Z_L}{Z_o} = \frac{Ae^{-nL} + Be^{nL}}{Ae^{-nL} - Be^{nL}} \tag{23}$$

from which

$$(Z_o - Z_L)Ae^{-nL} + (Z_o + Z_L)Be^{nL} = 0 \ . \tag{24}$$

Evaluating $\bar{H}$ at x = 0

$$\bar{H}(0,s) = A + B \ , \tag{25}$$

therefore

$$(Z_o - Z_L)(\bar{H}(0,s) - B)e^{-nL} + (Z_o + Z_L)Be^{nL} = 0 \ , \tag{26}$$

and

$$B = \frac{\bar{H}(0,s)}{1 - \left(\frac{Z_o+Z_L}{Z_o-Z_L}\right) e^{2nL}} \ . \tag{27}$$

From equation 25 then

$$A = \frac{\bar{H}(0,s)}{1 - \left(\frac{Z_o-Z_L}{Z_o+Z_L}\right) e^{-2nL}} \ . \tag{28}$$

Letting

$$k = \frac{Z_o - Z_L}{Z_o + Z_L} \ , \tag{29}$$

equation 17 becomes

$$\bar{H}(x,s) = \bar{H}(0,s) \ \frac{e^{-nx} - ke^{-n(2L-x)}}{1 - ke^{-2nL}} \ . \tag{30}$$

Evaluating equation 30 at x = L and dividing through by $\bar{H}(0,s)$

$$\frac{\bar{H}(L,s)}{\bar{H}(0,s)} = \bar{W}(s) = \frac{(1 - k)e^{-nL}}{1 - ke^{-2nL}} \ . \tag{31}$$

When the numerator is divided by the denominator in equation 31

$$\bar{W}(s) = (1 - k) \sum_{m=1}^{\infty} k^{(m-1)} e^{-(2m-1)nL} . \tag{32}$$

From equation 14

$$n = \frac{s}{a} \sqrt{1 + \frac{Fg}{s}} \ . \tag{33}$$

Applying the binomial expansion to equation 33 and neglecting

all but the first two terms, yields

$$n = \frac{s}{a} + \frac{Fg}{2a} \quad . \tag{34}$$

This expansion will converge for $\frac{Fg}{s}$ less than 1, therefore $|s|$ must be greater than Fg. Considering only the imaginary part of the complex variable s, this means that the approximation may be reasonable for frequencies greater than Fg. Equation 32 then becomes

$$\overline{W}(s) = (1 - k) \sum_{m=1}^{\infty} k^{(m-1)} e^{-(\frac{2m-1}{2a})FgL} \; e^{-(\frac{2m-1}{a})Ls} \quad . \tag{35}$$

The friction factor "F" has been assumed constant throughout this derivation. According to equation 35, attenuation due to friction would be the same for all frequencies. It has been stated (19, 20, 21) that this is not the case, so an attempt was made to approximate actual conditions. Binder's analysis of the friction factor gave F as a function of the properties of the fluid and frequency of pressure disturbance. The expression he gave, modified to have consistent dimensions with the friction factor in equation 35 is

$$F = \frac{2}{Dg} \left[\frac{\omega}{\rho\pi}(\mu + \epsilon + \frac{k_t}{c_p})\right]^{\frac{1}{2}} , \tag{36}$$

or

$$F = \beta \omega^{\frac{1}{2}} \tag{37}$$

where β incorporates the constants in equation 36. The attenuation due to friction in equation 35 would appear as

$$\exp\left[\frac{-(2m-1)\beta g L \omega^{\frac{3}{2}}}{2a}\right], \tag{38}$$

or

$$\exp\left[-(2m-1)(\alpha^2\omega)^{\frac{3}{2}}\right] \tag{39}$$

where α incorporates the constants in equation 38. For m = 1, equation 39 would be

$$\exp\left[-(\alpha^2\omega)^{\frac{3}{2}}\right] . \tag{40}$$

In the field of control theory a familiar graphical means of displaying functions of frequency is the Bode plot (30). The Bode plot of 40, which has the coordinates decibel (db) vs. log $(\alpha^2\omega)$ appears as in Figure 1, where

$$db = 20\log \exp\left[-(\alpha^2\omega)^{\frac{3}{2}}\right] = \frac{-20(\alpha^2\omega)^{\frac{3}{2}}}{\ln 10} = -\Gamma\omega^{\frac{3}{2}} \tag{41}$$

and

$$\Gamma = \frac{20\alpha}{\ln 10} . \tag{42}$$

It appeared from this curve that this function could be approximated by a first order lag system of the form

$$\frac{\omega_n}{s + \omega_n} \tag{43}$$

which would have a straight line asymptote of db = 0 from $\omega = 0$ to $\omega = \omega_n$, and an asymptote with slope of -20 db per decade from $\omega = \omega_n$ to $\omega = \infty$. The actual curve of equation 43 would be down 3 db at the breakpoint $\omega = \omega_n$ from the asymptotes.

One possible approximation was then found by fitting the asymptotes of equation 43 tangent to the curve of equation 41.

Figure 1. Bode plot of Equation 40

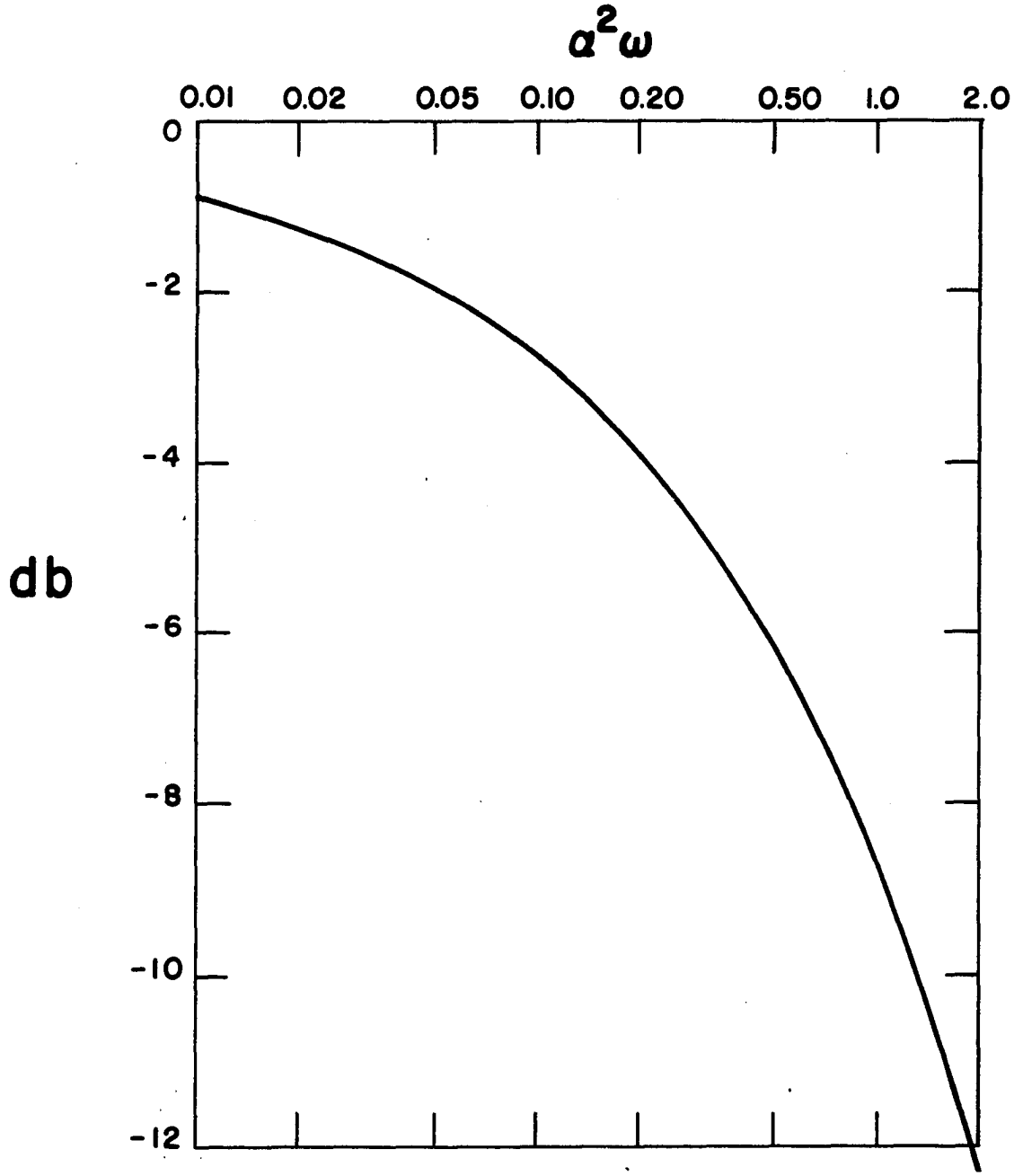
$\alpha^2\omega$
0.01
0.02
0.05
0.10
0.20
0.50
1.0
2.0
0
-2
-4
-6
-8
-10
-12
db

The point of tangency was found where the slope of 41 was -20 db per decade,

$$\frac{d(db)}{d(\log\omega)} = -20 = \frac{-\Gamma\omega^{\frac{1}{2}}}{2}\ln 10 \quad , \tag{44}$$

and solving for ω and db at this point

$$\omega = \frac{4}{\alpha^2} \qquad \text{and db} = -\frac{2\Gamma}{\alpha} \tag{45}$$

To find ω_n for this approximation, the assumed asymptote was extrapolated to db = 0 by

$$\frac{0 - (-2\Gamma/\alpha)}{\log\omega_n - \log 4/\alpha^2} = -20 \quad . \tag{46}$$

Solving 46 for ω_n gave

$$\omega_{n_1} = \frac{0.543}{\alpha^2} \tag{47}$$

but, according to equation 41, the attenuation at this break-point frequency was actually 6.4 db, which is over twice that of the first order approximation.

Another possible approximation was found by making ω_n the frequency at which the attenuation of equation 41 was 3 db. This was

$$\omega_{n_2} = \frac{0.1195}{\alpha^2} \quad . \tag{48}$$

The first approximation would give better accuracy for frequencies greater than ω_n, and the second approximation better accuracy for frequencies less than ω_n. The choice of either of these or any of the many more possibilities would depend on the value of α and the frequencies of interest.

Incorporating equation 43 for the friction dissipation

into equation 35 gives

$$\bar{W}(s) = (1-k) \sum_{m=1}^{\infty} k^{(m-1)} \left(\frac{\omega_n}{s+\omega_n}\right)^{(2m-1)} \exp\left[\frac{-(2m-1)Ls}{a}\right] \quad (49)$$

Since the exponential term of this equation is a dead time or delay, a qualitative description of the output pressure would be:

$\frac{L}{a}$ seconds after a pressure disturbance is initiated at the input of the line this disturbance appears at the output, modified by the friction dissipation. Also at this time a pressure equal to a minus k times the input disturbance and modified by the friction term is superimposed on the original wave. This total pressure wave is then reflected up the line and back to the load, being modified by the friction term both up and back. $\frac{2L}{a}$ seconds later it has returned, and a pressure of k times this wave is superimposed on the existing pressure at the load. This process continues indefinitely, or until it has damped out.

It should be noted that the incorporation of equation 43, the first-order representation for friction, into equation 35 is only an attempt to approximate effects of friction as a function of frequency. Accurate accounting would require that this effect should be introduced into equation 5, which would result in a nonlinear equation presently insoluble.

EXPERIMENTAL STUDY OF FLUID TRANSMISSION LINE BEHAVIOR

Experimental Equipment

Figure 2 is a diagram of the experimental apparatus used in this investigation. The line used in the experiment was a 2.073-inch inside-diameter aluminum tube with a 0.148-inch wall thickness. The length between transducer stations was 20.16 feet and was supported by rollers every five feet over the center span. Each end rested on a resilient material which allowed axial freedom of motion.

The fluids used in the two groups of tests were ethyl alcohol and distilled water, respectively.

The steel input-block shown in Figure 3 contained the upstream pressure transducer and the disturbance generator. The block was made large to provide an essentially rigid body as compared to the tube, and to provide the capabilities for possible use with a flow experiment at a later date. The unused interior was filled with a steel plug which extended almost to the transducer pressure port. The disturbance generator consisted of a piston which was pulsed by a pendulum or moved by hand. A spring was used to return the piston for a shorter pulse duration. The sealing of the piston was accomplished by a Bellofram rolling diaphragm which had negligible friction. The effective area of the piston was 0.64 square inches.

Figure 2. Diagram of experimental apparatus

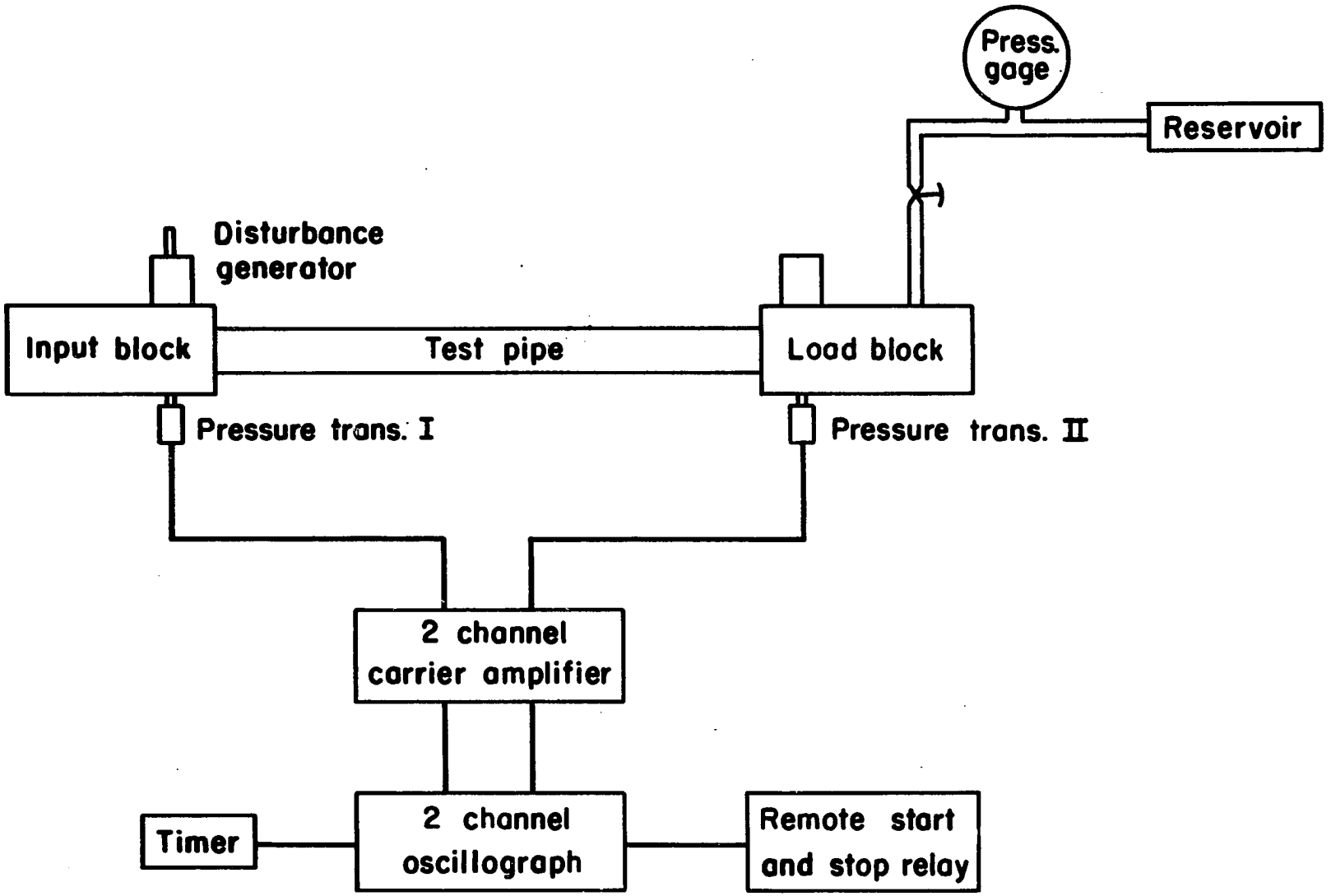
Press. gage
Reservoir
Disturbance generator
Input block
Test pipe
Load block
Pressure trans. I
Pressure trans. II
2 channel carrier amplifier
Timer
2 channel oscillograph
Remote start and stop relay

Figure 3. Input block

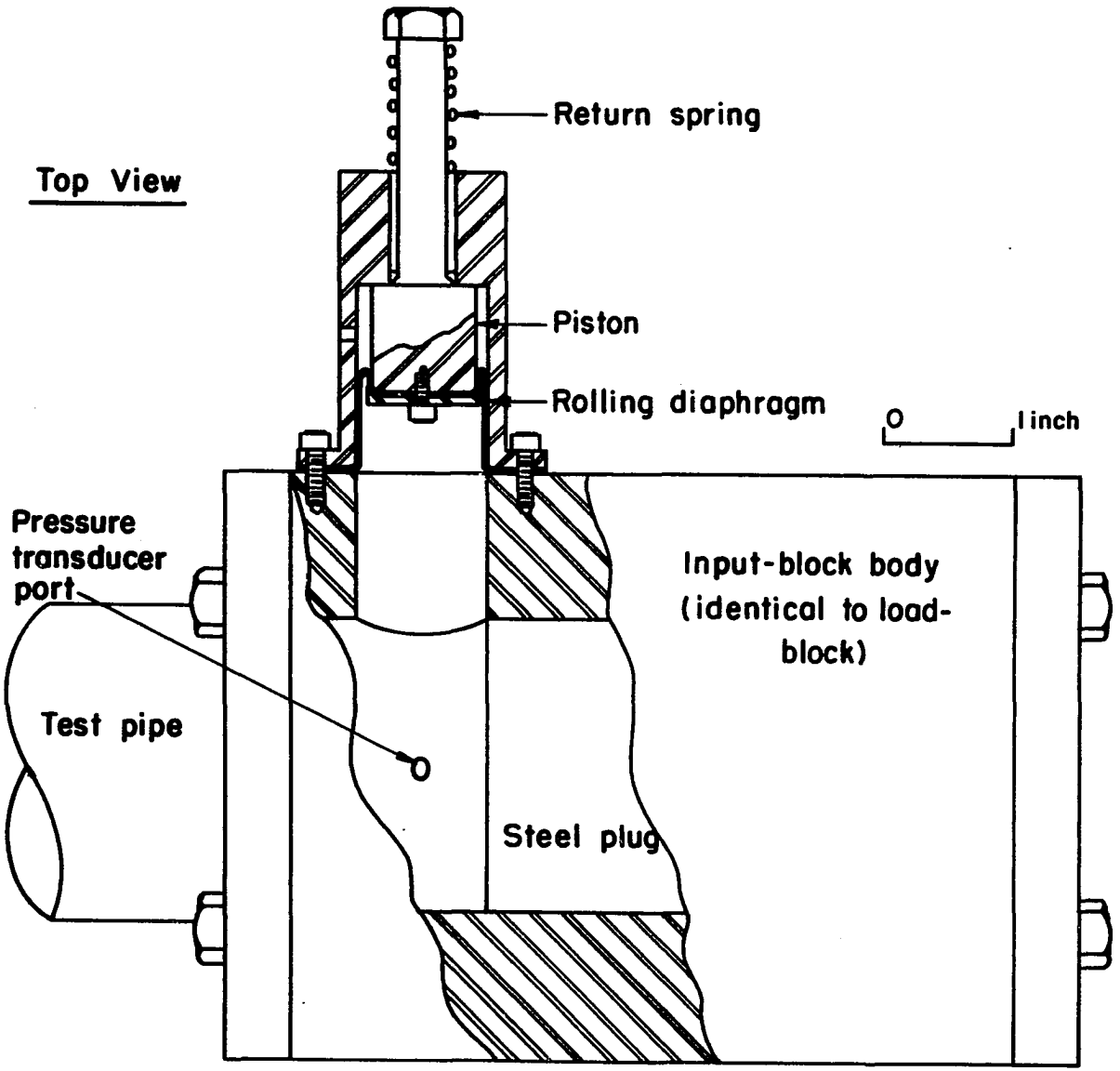
Top View
Return spring
Piston
Rolling diaphragm
0
1 inch
Pressure transducer port
Test pipe
Input-block body (identical to load-block)
Steel plug

The output or load-block shown in Figure 4 contained the downstream pressure transducer and was either completely dead-ended for infinite impedance or had a 0.312-inch inside-diameter mounted glass tube which contained a predetermined air space for a calculated capacitive impedance. When the tube was used dead-ended, a piston-cylinder reservoir supplied make-up fluid and applied initial pressure to the tube. A bourdon-tube pressure gage indicated the pressure in the reservoir, and a valve was used to isolate the reservoir from the tube. The reservoir and attached gage were connected to the load-block by means of a rubber tube to eliminate vibrations due to cantilever-supported masses. When the glass capacitance tube was used, initial pressure was introduced by a piston arrangement in the load-block which was identical to that in the input-block. This piston had originally been designed into the apparatus to give the capacitive load, but it was found that the inertia and friction effects were too large to be neglected. It was also discovered that the ability to easily vary the static pressure was necessary, because the temperature coefficient of pressure in the tube was about 3 psi/^{o}F. This meant, too, that the tube had to be vented when not in use to protect the transducers and seals from possible overpressure caused by a large ambient temperature change.

The transducers were Statham Instruments, Inc., full

Figure 4. Load block (Capacitor tube installed)

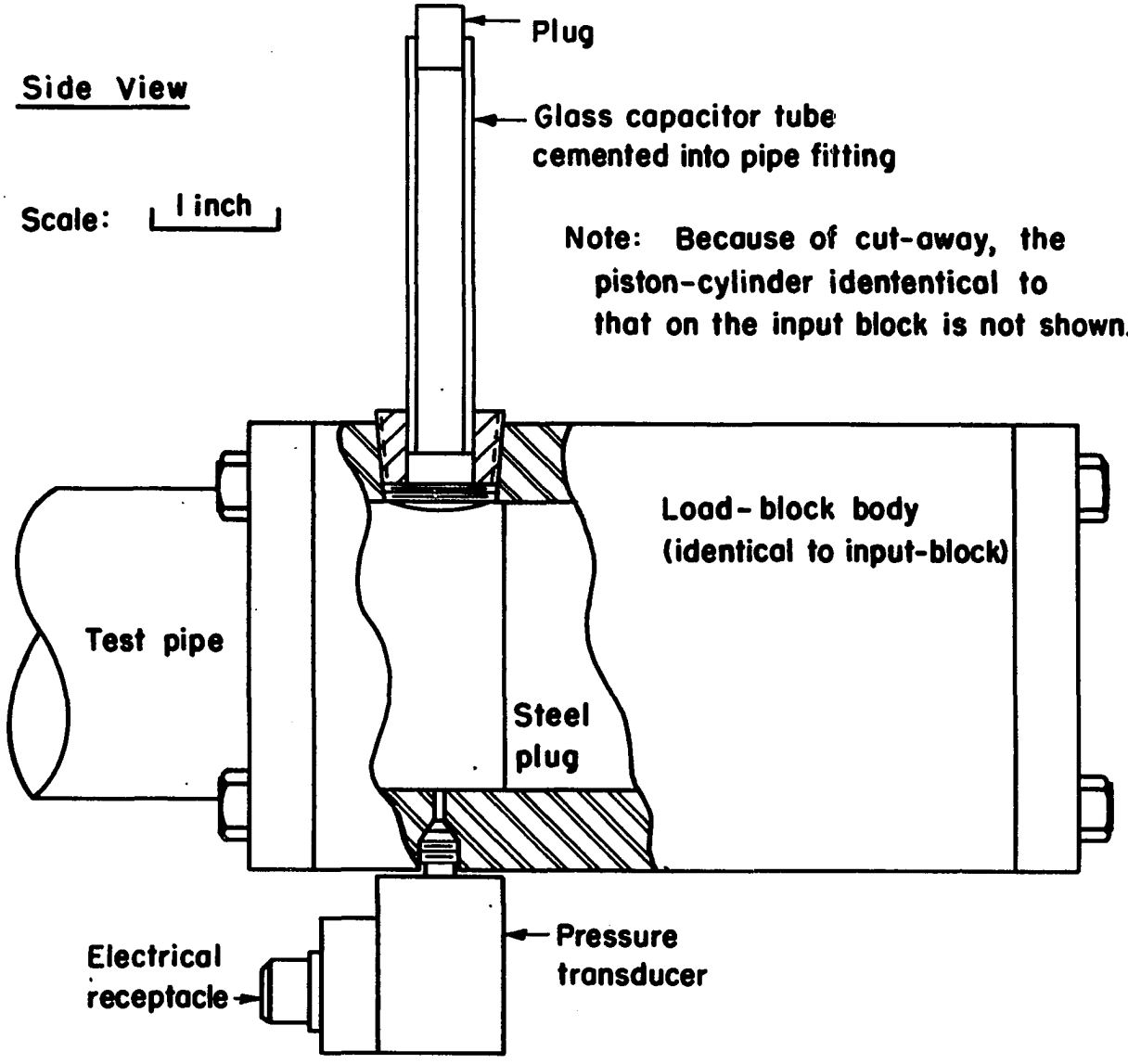
Side View
Scale: 1 inch
Plug
Glass capacitor tube cemented into pipe fitting
Note: Because of cut-away, the piston-cylinder idententical to that on the input block is not shown.
Load-block body (identical to input-block)
Test pipe
Steel plug
Electrical receptacle
Pressure transducer

bridge, temperature-compensated, commercial strain-gage types, models PA295TC (output) and PA183TC (input) with a pressure range of 0 - 100 psia. The natural frequency of the transducers was approximately 10,000 cycles per second. The transducers were used in conjunction with a Minneapolis-Honeywell Regulator Company Model 130-2C Carrier Amplifier and Heiland Model 906B Visicorder light beam oscillograph. The combined frequency response of the amplifiers and galvanometers was 1000 cycles per second. The maximum chart speed of the oscillograph was 50 inches per second. The chart drive was controlled by a remote switch in conjunction with a time delay relay which stopped the drive after approximately one second of running time for purposes of conserving recording paper. An auxiliary timing unit was available to give timing marks of 1, 0.1 or 0.01 seconds on the chart.

A continuous record of the temperature of the tube was made by means of an iron-constantan thermocouple and a Leeds and Northrup continuous strip-chart recording potentiometer.

Procedure

Calibrations were first made on all pieces of equipment. The two pressure transducers and the bourdon-tube gage were calibrated against a dead-weight tester, and it was determined that the linearity of the transducers was within the 0.75 per cent of full scale specified by the manufacturer. The timing

unit was calibrated against an electronic counter and adjusted to within 0.2 per cent accuracy when operating with a 0.01 second period.

Before each series of data runs, the pressure sensing system was balanced at atmospheric pressure. This system included the transducers, amplifiers and oscillograph. The sensitivity for both channels was set by internal calibration in the amplifiers. An initial pressure was introduced into the tube to insure that the lowest transient pressure would not approach the vapor pressure of the fluid. A check was then made on the oscillograph to see that both light beams had deflected equal distances. This check was the most important calibration, because the results depended on the comparison of the change in pressure at the two ends of the tube.

The chart drive speed was set at 50 inches per second, and the drive started by the remote switch. The pressure disturbance was introduced at the input end of the tube when the chart drive was up to speed, and the drive was automatically stopped by the time-delay relay after the transients had died out sufficiently.

A series of four or five runs were made at each condition of load impedance and for each fluid (see Table 1). An attempt was made to introduce a short pulse as one type of input waveform. A pulse width of about 0.004 seconds was obtained with the pendulum hammer. Other wave forms were introduced by hand.

After each run a reading of the temperature was taken.

The runs with a pulse input were used to determine the elapsed time between input pulse and received signal at the load end. In the interests of accuracy, more slowly varying inputs were used to determine the transfer function.

Data Reduction

The transfer function for each fluid and load condition was achieved in the following manner:

Values of both the input and output pressures were read every 0.002 seconds from the oscillograph record with the first reading taken when the input pressure first deviated from its initial steady-state value.

The Laplace transforms of both the input and output pressures were taken on a digital computer by the numerical procedure outlined in Appendix C. The transfer function for each run was then found by dividing the output transform by the input transform. The average for all runs within a series for a given fluid and load impedance was found by dividing the summation of output transforms by the summation of input transforms. The principle of superposition dictated this method for finding the average in preference to taking the average of the individual transfer functions.

Results

Five series of runs were made with the following conditions in Table 1, where P_o is the steady-state absolute pressure in the pipe, l_o is the height of the column of trapped air in the capacitor and Z_L is the load impedance. Reference is made to Appendix E for calculation of the capacitor impedance, $Z_L = C/s$.

Table 1. Test conditions

Series	Fluid	Type of load	P_o, psia	l_o, inches	Z_L sec	Temp., F
1	Alcohol	Dead end	28.7	-	∞	78
2	Alcohol	Capacitive	17.2	2.25	16,600/s	78
3	Alcohol	Capacitive	23.0	1.50	33,200/s	78
4	Water	Capacitive	21.2	1.80	20,200/s	78
5	Water	Dead end	24.7	-	∞	76

Table 2 lists the observed velocity of the pressure wave for the five series of runs, where P_p is the absolute pressure of the pulse used to obtain a_o, the observed velocity of the pressure wave in the pipe, and a_c is the theoretical wave velocity computed from equation B-22, Appendix B.

Table 2. Theoretical and observed wave velocities

Series	P_p, psia	a_o, fps	a_c, fps
1	37.7	3720	3254
2	23.2	3640	3254
3	30.8	3610	3254
4	29.5	4440	3970
5	43.5	4300	3970

The value of k, the reflection coefficient, was computed in the following manner.

For $Z_L = \infty$

$$k = \frac{Z_o - Z_L}{Z_o + Z_L} = -1 \quad . \tag{50}$$

For $Z_L = C/s$, referring to equation 20,

$$k = \frac{\frac{a}{g}\sqrt{1 + \frac{Fg}{s}} - \frac{C}{s}}{\frac{a}{g}\sqrt{1 + \frac{Fg}{s}} + \frac{C}{s}} \quad . \tag{51}$$

If the binomial expansion of the radical is used as was done in equation 33 then

$$k = \frac{s - \left(\frac{Cg}{a} - \frac{Fg}{2}\right)}{s + \left(\frac{Cg}{a} + \frac{Fg}{2}\right)} \quad , \tag{52}$$

but

$$\frac{Cg}{a} \gg \frac{Fg}{2} \tag{53}$$

for frequencies of interest, so that

$$k = \frac{s - \frac{Cg}{a}}{s + \frac{Cg}{a}}$$

as a good approximation.

ω_n was computed as the log mean of ω_{n_1} equation 47 and ω_{n_2} equation 48. This gives

$$\omega_n = \frac{0.258}{\alpha^2} \cdot \tag{54}$$

Table 3 lists the values of the properties of alcohol and water that were used to calculate the friction factor F, load impedance Z_L and theoretical wave velocity a_c. The eddy viscosity term ϵ was assumed zero for lack of published data. The modulus of elasticity for aluminum was taken as 10.2×10^6.

Table 3. Fluid properties

	Alcohol	Water	Reference
lb μ - sec/ft^2	2.4×10^{-5}	2.0×10^{-5}	(31, p. 8)
slugs/ft^3 ρ	1.53	1.94	(32, p. 485)
B.T.U./sec - ft^2-^{o}F/ft k_t	2.778×10^{-5}	9.72×10^{-5}	(33, p. 17)
B.T.U./lb$_m$-^{o}F c_p	0.58	1.0	(33, p. 10)
lb/in.^{2} K	175,000	312,000	(32, p. 485)
lb/ft^3 w	49.3	62.4	(32, p. 485)

Figure 5 shows a typical record of input and output pressures for a run from series number 2. This is a replot of the original oscillograph record.

Figures 6 through 10 are plots of the experimental $\bar{W}(s)_{ave.}$ vs. s for series 1 through 5 respectively. Also plotted are curves of $\bar{W}(s)$ from the analytical expression 49 using both the calculated value of a_c from equation B-22, Appendix B, and the observed value a_o from Table 2.

It was discovered that a calibration error existed in some of the runs which may have been caused by amplifier drift. The plotted experimental curves in Figures 6 through 10 have been corrected to account for this error.

Figure 5. Input and output pressures versus time for a run from series number 2

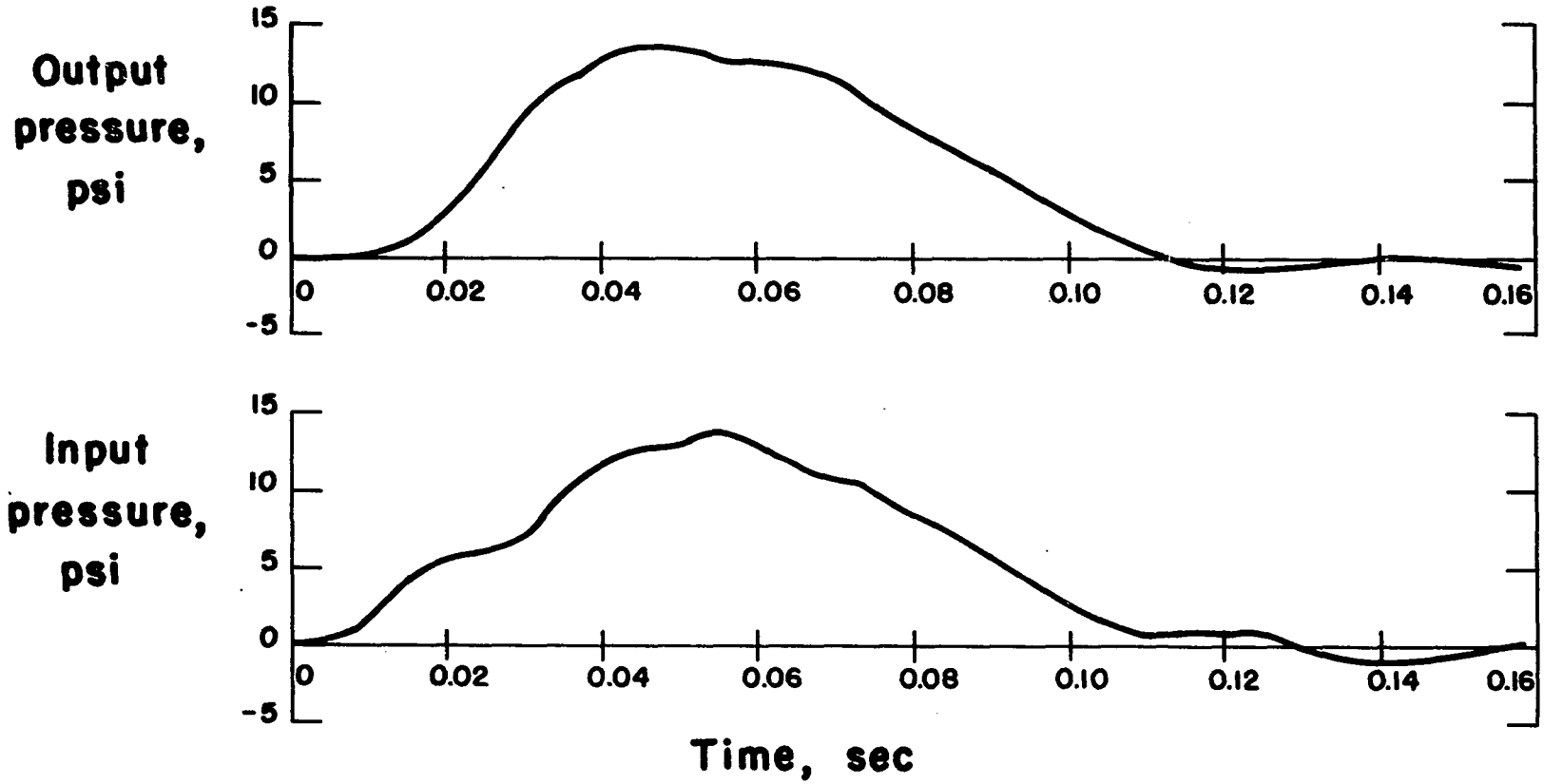
Output pressure, psi
15
10
5
0
-5
0
0.02
0.04
0.06
0.08
0.10
0.12
0.14
0.16
Input pressure, psi
15
10
5
0
-5
0
0.02
0.04
0.06
0.08
0.10
0.12
0.14
0.16
Time, sec

Figure 6. Transfer function for test series number 1

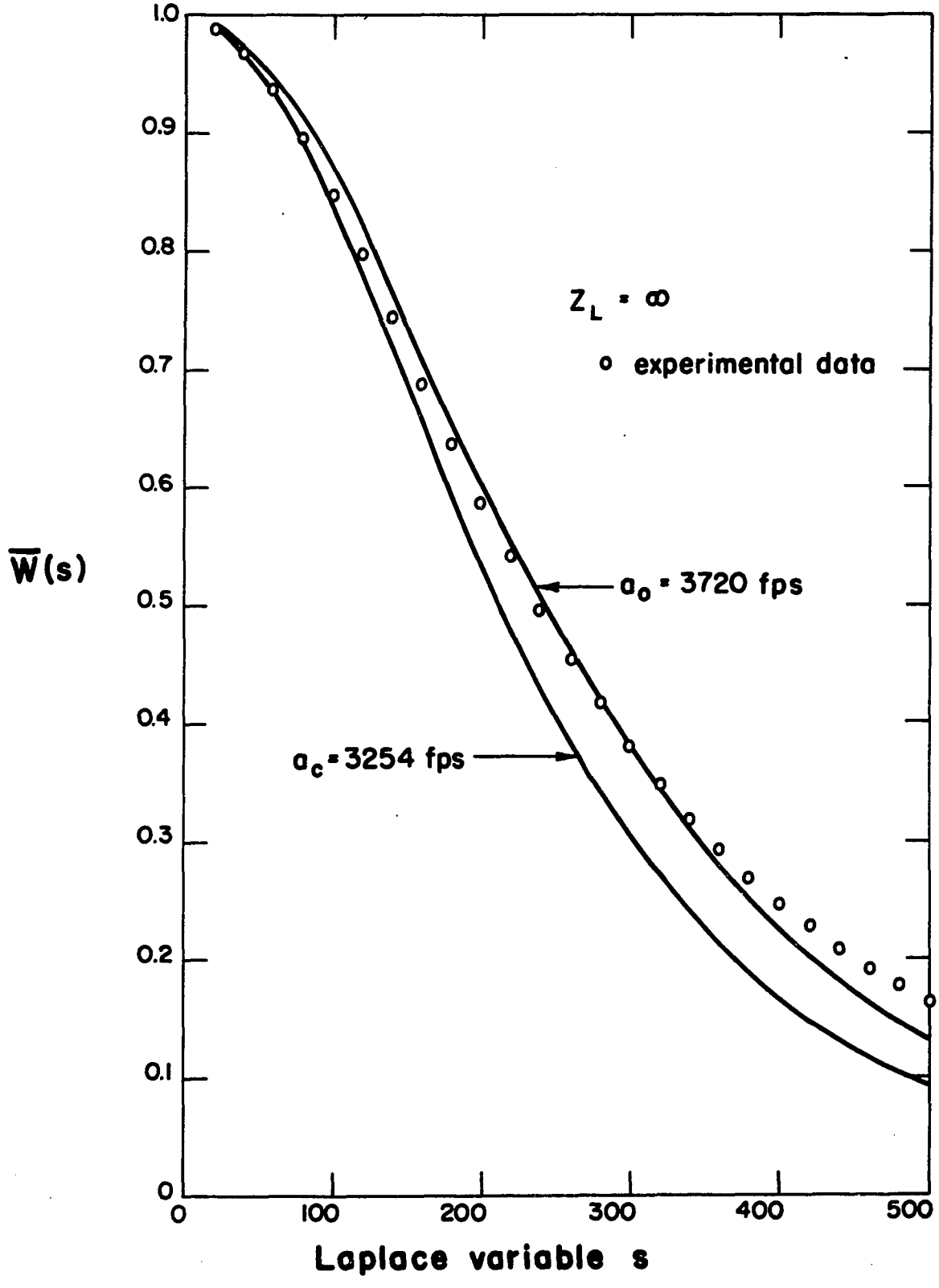
1.0
0.9
0.8
0.7
0.6
0.5
0.4
0.3
0.2
0.1
0
0
100
200
300
400
500
$\overline{W}(s)$
Laplace variable s
$Z_L = \infty$
o experimental data
a_o = 3720 fps
a_c = 3254 fps

Figure 7. Transfer function for test series number 2

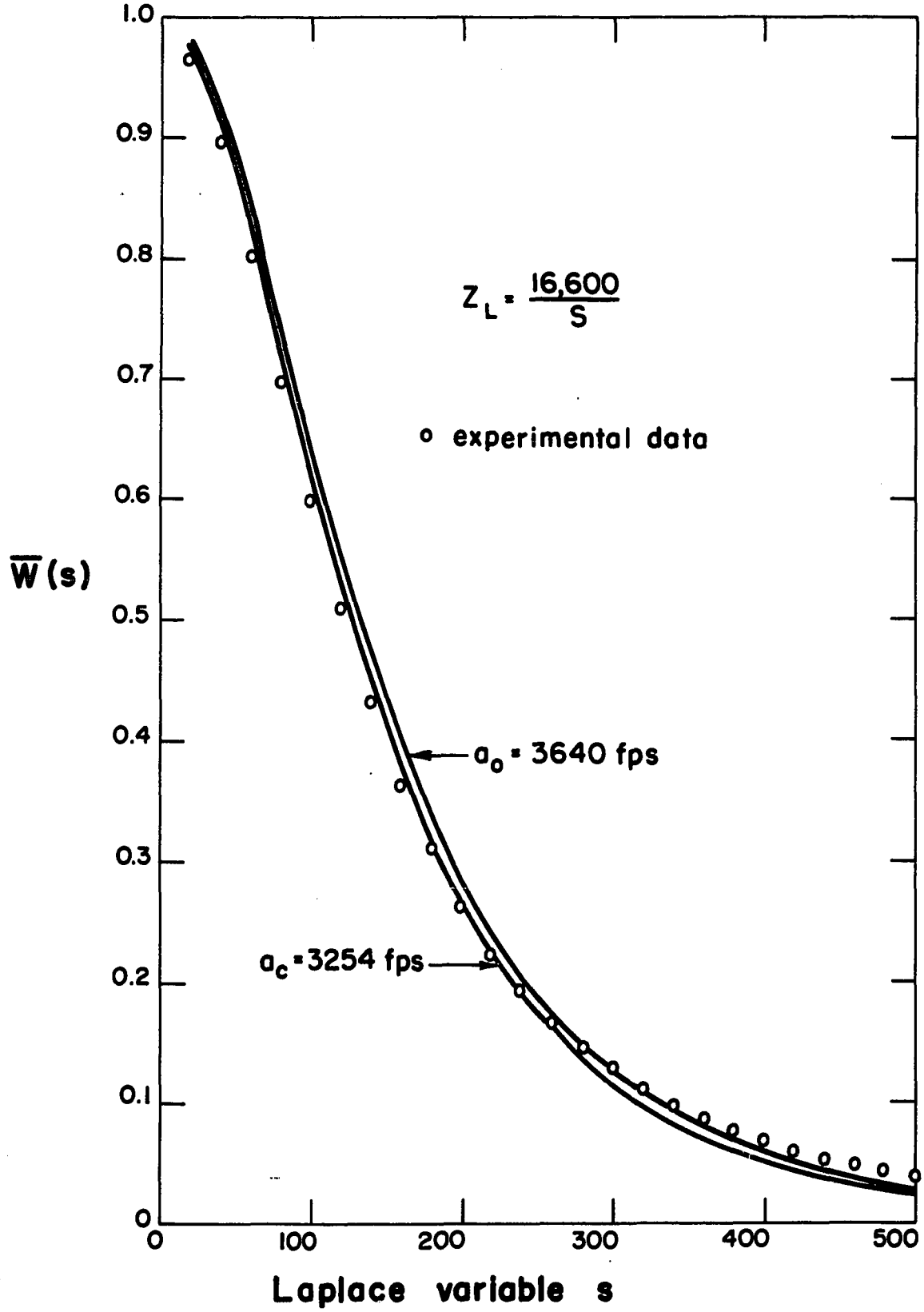
1.0
0.9
0.8
0.7
0.6
0.5
0.4
0.3
0.2
0.1
0
$\overline{W}(s)$
$Z_L = \frac{16,600}{S}$
o experimental data
a_o = 3640 fps
a_c = 3254 fps
0
100
200
300
400
500
Laplace variable s

Figure 8. Transfer function for test series number 3

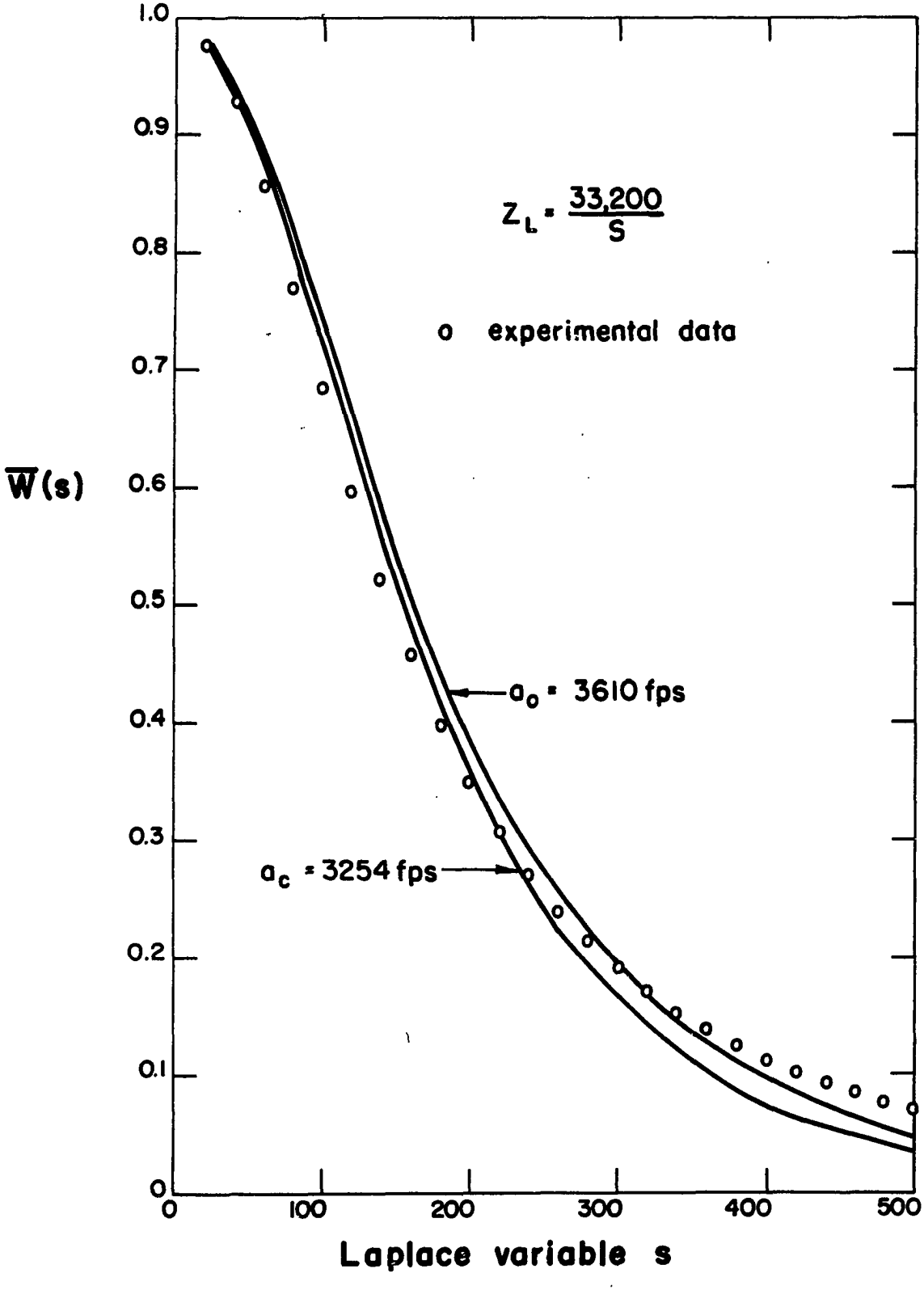
1.0
0.9
0.8
0.7
0.6
0.5
0.4
0.3
0.2
0.1
0
$\overline{W}(s)$
$Z_L = \frac{33,200}{S}$
o experimental data
a_o = 3610 fps
a_c = 3254 fps
0
100
200
300
400
500
Laplace variable s

Figure 9. Transfer function for test series number 4

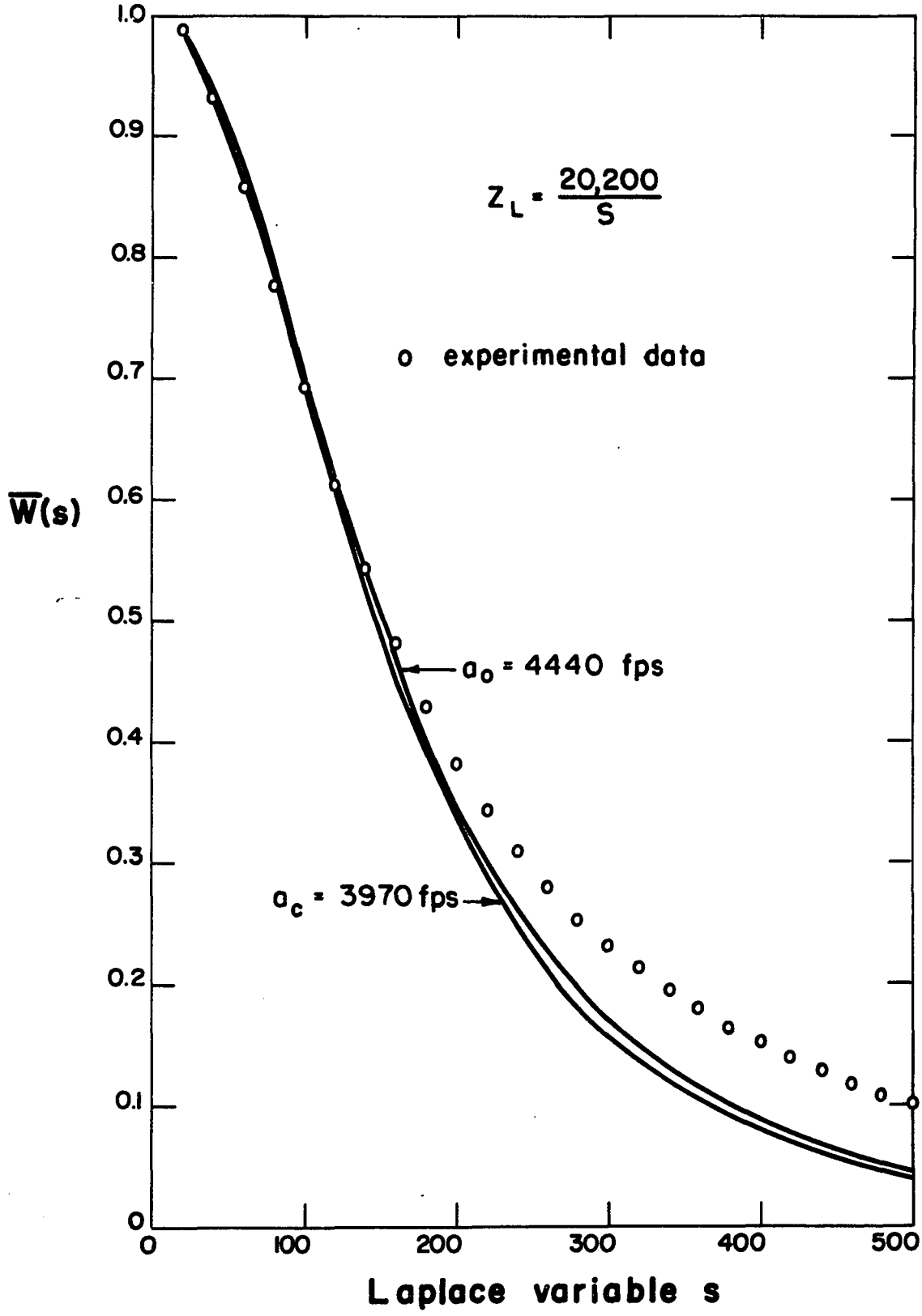
1.0
0.9
0.8
0.7
0.6
0.5
0.4
0.3
0.2
0.1
0
$\overline{W}(s)$
$Z_L = \frac{20,200}{S}$
o experimental data
a_o = 4440 fps
a_c = 3970 fps
0
100
200
300
400
500
Laplace variable s

Figure 10. Transfer function for test series number 5

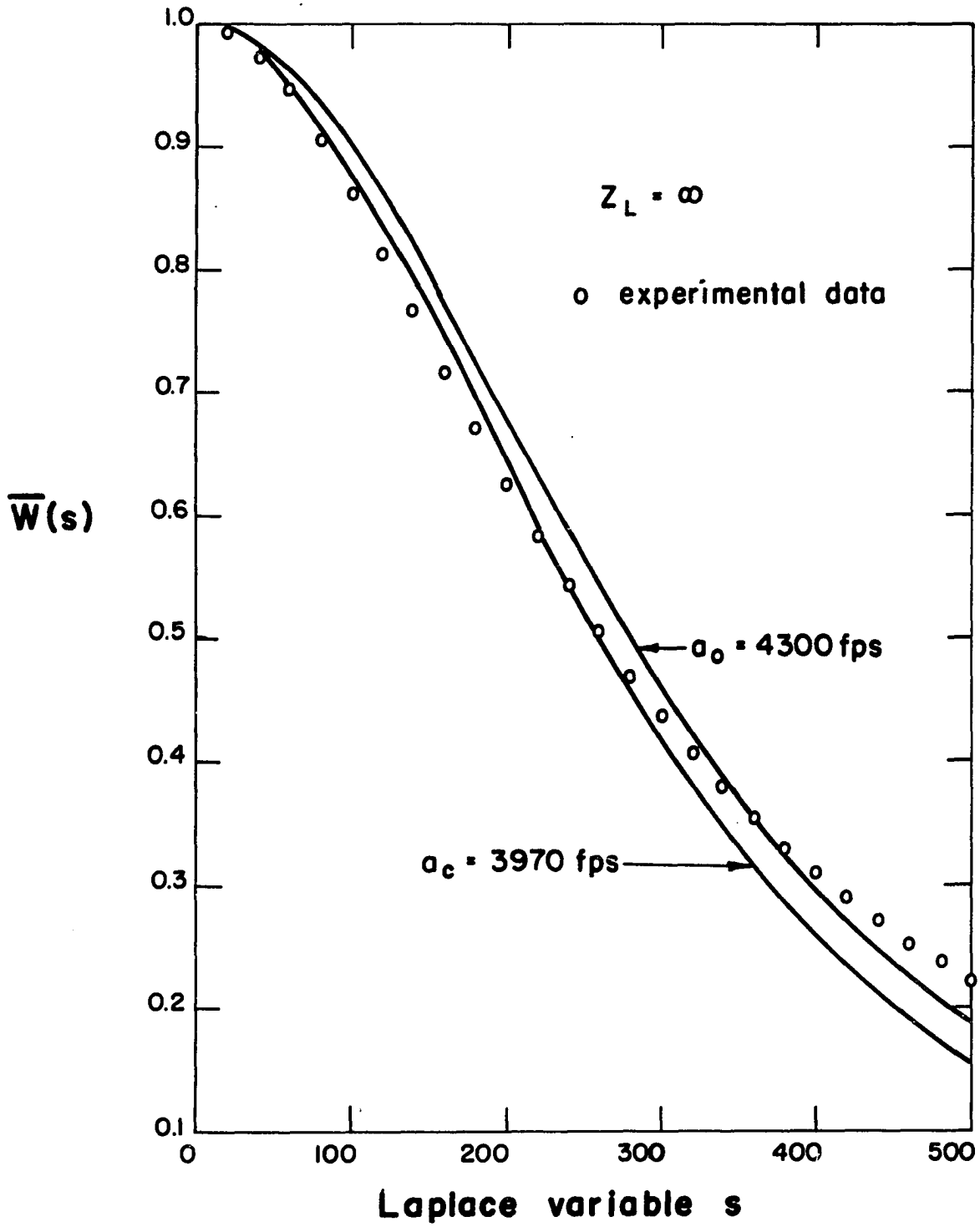
1.0
0.9
0.8
0.7
0.6
0.5
0.4
0.3
0.2
0.1
0
100
200
300
400
500
$\overline{W}(s)$
$Z_L = \infty$
o experimental data
a_o = 4300 fps
a_c = 3970 fps
Laplace variable s

DISCUSSION OF RESULTS

Reference is made to Figures 6 through 10. It will be noted that all the theoretical transfer function curves computed from equation 49 follow the general trend of their respective experimental transfer function curves. Therefore it can be concluded that the transfer function denoted by equation 49 is a reasonable representation of the physical system.

The largest difference in all sets of curves occurs at large values of s. This discrepancy may be partly due to the method of taking the experimental transfer function on the digital computer. Because the continuous data was necessarily digitalized, the exact value of dead time between input and output pressure waves would not be recognized by the computer unless it be by chance that the dead time was a multiple of the time increment used. This did not occur during this investigation. The computer check problem used in Appendix C was deliberately chosen as an attempt to match this condition. It will be noted that the greatest percentage error occurs at large values of s here, too.

The curves computed using the observed wave velocity, a_o, follow more closely the experimental curves than those using the theoretical velocity, a_c. Table 2 shows a 10 to 15 per cent difference between these values of wave velocity. A possible cause of this difference might be the large pressure

gradient of the input pulse used to measure wave velocity. The pressure waves used to compute the experimental transfer functions displayed a smaller pressure gradient than those runs that were made to measure the wave velocity, but still, the pressure front was relatively steep, and therefore may exhibit this error. These data-run records could not be measured accurately for the dead time because of the relatively slow rise time of the pressure wave form.

The deviations between theoretical and experimental results were caused by many factors, probably the most significant of these being the assumptions made when deriving the theoretical transfer function. Some of these are: 1) a first-order time-constant element approximation for the friction effect; 2) a two-term binomial expansion of the radical appearing in n, the pipe characteristic variable; 3) a linear approximation for the capacitor impedance; and 4) a two-term binomial expansion of the radical appearing in Z_o, the pipe characteristic impedance.

The calibration of the transducer system depended on the setting of two light beams, each of which, when at rest, had a relatively wide image. This wide image was necessary so that there would be enough intensity to give a trace at fast writing speeds. Calibration errors did exist here, but were detected when processing the data and corrected.

The digitalization of the data was accomplished within $\pm$ 0.2 psi for pressure and $\pm$ 0.0005 seconds for time. Inac-

curacies in this procedure would tend to smooth out in the integration when taking the transform.

Because both transducer channels had similar components, inaccuracies of the pressure readings due to frequency response characteristics of the transducer system would cancel upon taking the ratio of the transforms.

It is possible that a numerical procedure for taking the transforms using Simpson's rule instead of the trapezoidal rule used would give better results. Also, a computer program recognizing the exact dead time might have been more accurate.

This investigation confirmed the results of other investigators. First, the effect of friction in the no-flow case is small (26). Introducing more friction effect by decreasing ω_h actually causes a greater deviation between theoretical and experimental curves of the transfer function. The most efficient method to bring the curves in closer agreement would be to arrive at the best value of wave velocity. Second, if the line were terminated with an impedance equal to the line characteristic impedance, the reflected wave would disappear (4, 26). This fact is noted upon examination of the expression for k, the reflection coefficient. Third, for sharp wave fronts a small disturbance would travel down the pipe faster than the main wave (29). These precursor waves were noticed when using the pulse input.

CONCLUDING REMARKS AND RECOMMENDATIONS FOR CONTINUED INVESTIGATION

As was stated in the introduction, the purpose of this investigation was to arrive at the transfer function of a hydraulic transmission line. It was hoped that this transfer function could be readily programmed on an analog computer. By the use of certain approximations, the exact function given by equation 32 was modified to the form in equation 49. The analog computer simulation for this last function is given in Appendix D.

The experimental work was done to verify the validity of this function. This was done by means of a digital computer program that compared the experimental transfer function to that defined by equation 49 for a set of real, positive values of s. It was noted that the theoretical and experimental curves in general followed closely, and from this it was concluded that equation 49 was a reasonable representation of the system.

Admittedly, a much more reliable check on the validity and accuracy of the derived transfer function would have been to actually feed the experimental input wave forms into an analog computer programmed as in Appendix D and compare the output of the computer to the experimental output wave form. Such analog equipment was not available for this investigation.

This investigation was done only with a non-flow set-up.

Similar data should be taken with a flow system and these results checked against equation 35.

Further work should also be done to determine the reason for the discrepancy between the computed and observed wave velocities.

Finally, a suitable analytical approach recognizing nonlinear friction should be developed to avoid approximations such as that in equation 49.

REFERENCES

1. Paynter, Henry M. Fluid Transients in Engineering Systems. In Streeter, Victor L., ed. Handbook of Fluid Dynamics. 20-1 - 20-47. New York, N. Y., McGraw-Hill Book Co., Inc. 1961.

2. Lee, Y. C., Gore, M. R., and Ross, C. C. Stability and Control of Liquid Propellant Rocket Systems. Jet Prop. 23:75-81. 1953.

3. Sabersky, R. H. Effects of Wave Propagation in Fuel Feed Lines on Low-frequency Rocket Instability. Jet Prop. 24: 172-174. 1954.

4. Chang, S. S. L. Transient Effects of Supply and Connecting Conduits in Hydraulic Control Systems. Franklin Inst. J. 262:437-452. 1956.

5. Higgins, Thomas J. Electroanalogic Methods. III. App. Mechanics Rev. 10:49-54. 1957.

6. Paynter, H. M. Electrical Analogies and Electronic Computers: Surge and Water Hammer Problems. Amer. Soc. Civ. Engrs. Proc. 78, No. 146:1-28. 1952.

7. Sanders, John C., Novik, David, and Hart, Clint E. Effect of Dynamic Characteristics of Rocket Components on Rocket Control. Institute of the Aeronautical Sciences Preprint No. 710. 1958.

8. Reethof, G. Application of the Analog Computer to Predict Dynamic Performance in Typical Hydraulic Circuits. Amer. Soc. Mech. Engrs. Trans. 80:1299-1306. 1958.

9. Simin, O. Water Hammer. Amer. Water Works Assoc. Proc. 24:335-422. 1904.

10. LeConte, Joseph N. Experiments and Calculations on the Resurge Phase of Water Hammer. Amer. Soc. Mech. Engrs. Trans. 59:691-694. 1937.

11. Green, J. E. The Pressure Surge in Oil Pipe Lines. Third World Pet. Cong. Proc., The Hague. 9:7-21. 1951.

12. Rich, George R. Hydraulic Transients. New York, N. Y., McGraw-Hill Book Co., Inc. 1951.

13. Jaeger, Charles. Engineering Fluid Mechanics. London, England, Blackie and Son, Limited. 1956.

14. Parmakian, John. Waterhammer Analysis. New York, N. Y., Prentice-Hall, Inc. 1955.

15. Rich, G. R. Water Hammer Analysis by the Laplace-Mellin Transformation. Amer. Soc. Mech. Engrs. Trans. 67:361-376. 1945.

16. Binnie, A. M. The Effect of Friction on Surges in Long Pipelines. Qtrly. J. of Mechanics and App. Math. 4:330-343. 1951.

17. Rouleau, W. T. Pressure Surges in Pipelines Carrying Viscous Liquids. Amer. Soc. Mech. Engrs. Paper 60-Hyd-5. 1960.

18. Lieberman, P. and Brown, E. A. Pressure Oscillations in a Water-Cooled Nuclear Reactor Induced by Water-Hammer Waves. Amer. Soc. Mech. Engrs. Paper 60-Hyd-2. 1960.

19. Binder, R. C. Advanced Fluid Dynamics and Fluid Machinery. New York, N. Y., Prentice-Hall, Inc. 1951.

20. Binder, R. C. The Damping of Large Amplitude Vibrations of a Fluid in a Pipe. J. Acoust. Soc. Am. 15:41-43. 1943.

21. Brown, F. T. The Transient Response of Fluid Lines. Amer. Soc. Mech. Engrs. Paper 61-WA-143. 1961.

22. Wick, Robert S. An Analysis of Oscillatory Pressure in Liquid Propellant Rocket Systems and Application of the Analysis to Combustion Stability. California Institute of Technology, Jet Propulsion Laboratory Progress Report No. 20-231. ca. 1955. Original not available; cited in Sanders, John C., Novik, David, and Hart, Clint E. Effect of Dynamic Characteristics of Rocket Components on Rocket Control. Institute of the Aeronautical Sciences Preprint No. 710:15. 1957.

23. Keuger, P. Digital Computer Analysis of Transients in Liquid Rocket Systems. Jet Prop. 28:804-809. 1958.

24. Shearer, J. L. Conversion, Transmission, and Control of Fluid Power. In Streeter, Victor L., ed. Handbook of Fluid Dynamics. 21-1 - 21-54. New,York, N. Y., McGraw-Hill Book Co., Inc. 1961.

25. Li, Y. T. Stabilization of Low-Frequency Oscillations of Liquid Propellant Rockets with Fuel Line Stabilizer. Jet Prop. 26:26-33, 39. 1956.

26. Regetz, John D., Jr. An Experimental Determination of the Dynamic Response of a Long Hydraulic Line. Nat. Aero. and Space Admin. Tech. Note. No. D-576. 1960.

27. Lee, Y. C., Pickles, A. M. and Miesse, C. C. Experimental Aspects of Rocket System Stability. Jet Prop. 26:34-39. 1956.

28. Ezekiel, F. D. Effect of Conduit Dynamics on Control-Valve Stability. Amer. Soc. Mech. Engrs. Trans. 80: 904-908. 1958.

29. Skalak, R. An Extension of the Theory of Water Hammer. Amer. Soc. Mech. Engrs. Trans. 78:105-116. 1956.

30. Bode, H. W. Network Analysis and Feedback Amplifier Design. Princeton, N. J., D. Van Nostrand Co., Inc. 1945.

31. Streeter, Victor L. Fluid Mechanics. 2nd ed. New York, N. Y., McGraw-Hill Book Co., Inc. 1958.

32. Pao, Richard H. F. Fluid Mechanics. New York, N. Y., John Wiley and Sons, Inc. c 1961.

33. Knudsen, James G. and Katz, Donald L. Fluid Dynamics and Heat Transfer. New York, N. Y., McGraw-Hill Book Co., Inc. 1958.

ACKNOWLEDGMENTS

The author would like to express his appreciation for the guidance and advice received from Dr. G. K. Serovy, Dr. W. B. Boast, Dr. H. J. Weiss, Prof. H. M. Black and Dr. J. W. Nilsson of Iowa State University who served as the committee in charge of the author's graduate program. It has been a privilege to study under the direction of these gentlemen.

The President's Permanent Objective Committee, Iowa State University, through its financial support of the research, made possible the experimental investigation of the problem.

APPENDIX A - SYMBOLS AND NOTATION

A	area of pipe, ft^2
A	constant
A_c	area of fluid capacitor, ft^2
a_c	theoretical wave propagation velocity, ft/sec
a_o	observed wave propagation velocity, ft/sec
B	constant
C	constant
c	constant, dependent on end constraints of pipe
c_p	specific heat of fluid at constant pressure, BTU/lb
D	internal diameter of pipe, ft
D	constant
d	internal diameter of fluid capacitor, ft
db	decibel
E	modulus of elasticity, lb/ft^2
e	wall thickness of pipe, ft
e	base of Naperian logarithm
F	friction factor, sec/ft
g	gravitational constant, ft/sec^2
$\mathcal{H}$	total instantaneous pressure head, ft
H_o	steady-state pressure head, ft
H	perturbation pressure head, ft
$\overline{H}$	transformed perturbation pressure head
K	bulk modulus of fluid, lb/ft^2

k	reflection coefficient defined by equation 29
k_t	thermal conductivity of fluid, BTU/sec-ft-^oF
L	length of pipe, ft
l_o	initial height of air column in fluid capacitor, ft
ln	logarithm to base e
log	logarithm to base 10
m	summation index
n	summation index
n	pipe characteristic variable as defined by equation 14
n	isentropic constant exponent (Appendix E only)
P	pressure of air in fluid capacitor, lb/ft^2
R	internal radius of pipe, ft
R_L	resistive component of load impedance, sec
R_P	resistive component of pipe impedance, sec
s	Laplace variable, sec^{-1}
t	time, sec
$\mathcal{V}$	total instantaneous velocity, ft/sec
V_o	steady-state velocity, ft/sec
V	perturbation velocity, ft/sec
$\overline{V}$	transformed perturbation velocity, ft/sec
v	volume of trapped air in fluid capacitor, ft^3
$\overline{W}$	transfer function
w	specific weight of fluid, lb/ft^3
x	linear distance along pipe, ft
y	change in fluid capacitor surface level, ft

Z_L load impedance, sec

Z_o characteristic impedance of pipe, sec

α constant

β constant

Γ constant

ϵ eddy viscosity of fluid, lb - sec/ft^2

μ dynamic viscosity of fluid, lb - sec/ft^2

μ Poisson's ratio (Appendix B only)

ρ density of fluid, lb - sec^2/ft^4

ω frequency, rad/sec

ω_n breakpoint frequency, rad/sec

APPENDIX B - DERIVATION OF ONE-DIMENSIONAL DYNAMIC EQUATIONS (14)

Reference is made to the section entitled SYMBOLS AND NOTATION and Figure 11. It is assumed that:

a) The pipe remains full of fluid at all times, and the minimum pressure inside the pipe is in excess of the vapor pressure of the fluid.

b) The velocity head is negligible when compared with the pressure changes.

c) The velocity of fluid in the direction of the axis of the pipe is uniform over any cross section of the pipe.

d) The pressure is uniform over a transverse cross section of the pipe and is equal to the pressure at the center line of the pipe.

e) The effect of friction is a linear function of velocity.

An element of fluid which is bounded by two parallel faces normal to the axis of the pipe is considered. The condition of dynamic equilibrium requires that the unbalanced force acting on the element of fluid be made equal to the rate of change of momentum of the element; that is, Newton's second law of motion is satisfied.

It follows from the condition of dynamic equilibrium that

$$wHA - w(A+\frac{\partial A}{\partial x}dx)(H+\frac{\partial H}{\partial x}dx) - wAFVdx = \frac{w}{g}Adx\frac{dV}{dt}, \quad (B\text{-}1)$$

Figure 11. Differential fluid element

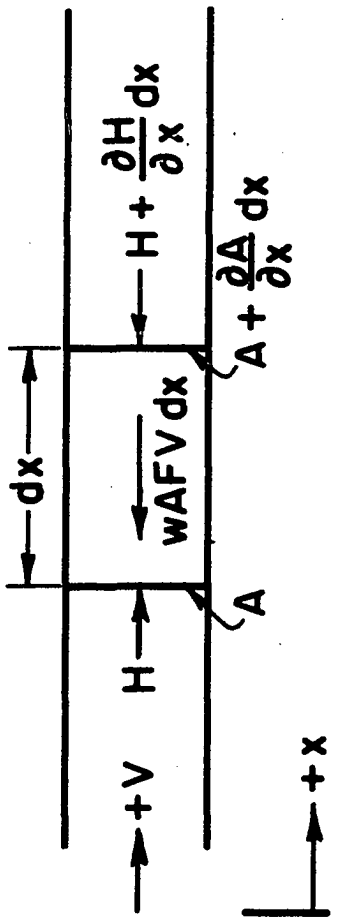
H + ∂H/∂x dx
A + ∂A/∂x dx
dx
wAFV dx
A
H
+V
+x

Neglecting terms of higher order, cancelling like terms and noting that

$$H \frac{\partial A}{\partial x} \ll A \frac{\partial H}{\partial x} \quad , \tag{B-2}$$

equation B-1 becomes

$$-wA \frac{\partial H}{\partial x} dx - wAFVdx = \frac{w}{g} Adx \frac{dV}{dt} \quad , \tag{B-3}$$

but

$$\frac{dV}{dt} = \frac{\partial V}{\partial t} + V \frac{\partial V}{\partial x} \quad , \tag{B-4}$$

therefore, introducing B-4 into B-1 and simplifying

$$- \frac{\partial H}{\partial x} = \frac{1}{g}\left(\frac{\partial V}{\partial t} + V \frac{\partial V}{\partial x}\right) + FV \quad . \tag{B-5}$$

A second equation relating H and V is determined from the condition of continuity. Referring to Figure 12, the average velocity of face B moving to D during the time interval dt is

$$V + \tfrac{1}{2} \frac{\partial V}{\partial x} \overline{BD} + \tfrac{1}{2} \frac{\partial V}{\partial t} dt \quad , \tag{B-6}$$

therefore

$$\overline{BD} = (V + \tfrac{1}{2} \frac{\partial V}{\partial x} \overline{BD} + \tfrac{1}{2} \frac{\partial V}{\partial t} dt)dt \quad . \tag{B-7}$$

Similarly

$$\overline{CF}=[V+ \frac{\partial V}{\partial x}dx + \tfrac{1}{2} \frac{\partial}{\partial x}(V+\frac{\partial V}{\partial x}dx)\overline{CF}+ \tfrac{1}{2} \frac{\partial}{\partial t}(V+\frac{\partial V}{\partial x}dx)dt]dt \quad . \tag{B-8}$$

Neglecting terms of higher order, then

$$\overline{BD} - \overline{CF} = - \frac{\partial V}{\partial x}dx \; dt \quad . \tag{B-9}$$

The change in length of the element dx is effected primarily by two factors. In the first place, a change in pressure causes the pipe shell to expand or contract. The resulting change in the cross-sectional area then produces a change

Figure 12. Velocities associated with fluid element

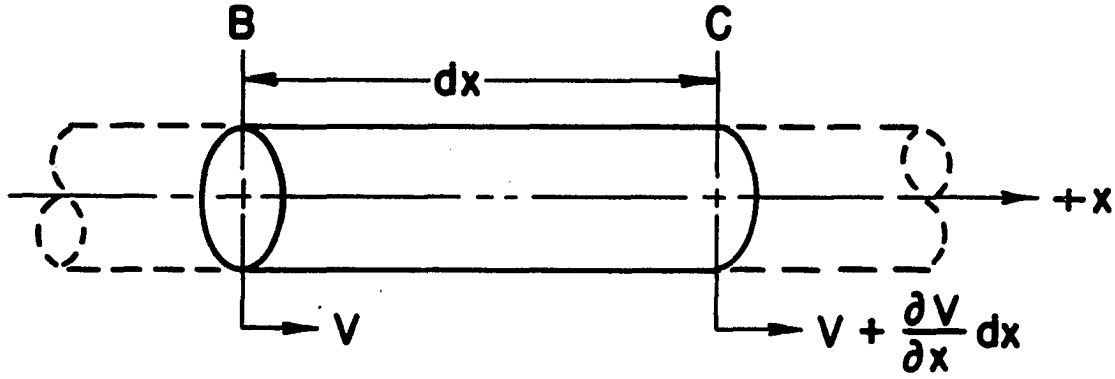

a) At time t

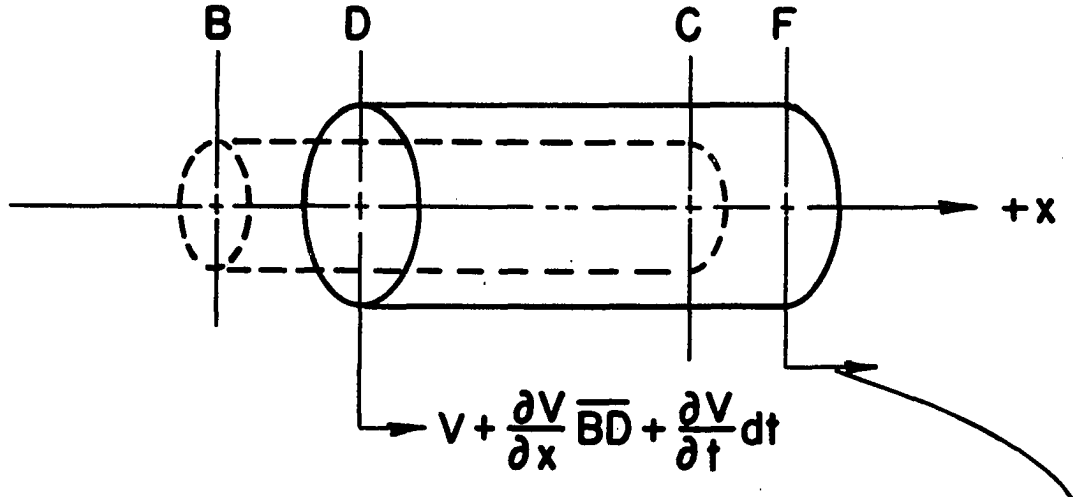

$$V + \frac{\partial V}{\partial x} dx + \frac{\partial}{\partial x} \left(V + \frac{\partial V}{\partial x} dx\right) \overline{CF} + \frac{\partial}{\partial t} \left(V + \frac{\partial V}{\partial x} dx\right) dt$$

b) At time t + dt

in the length of the element in order to contain the same volume of fluid. In the second place, because of the compressibility of the fluid, a change in pressure causes a change in the volume of fluid within the element, and as a consequence, a further change in the length of the element. Referring to Figure 13, the deformation of the element of the pipe shell produced by a change in the longitudinal and circumferential stresses is

$$\Delta R = \frac{R + e/2}{E} (\Delta\sigma_2 - \mu\Delta\sigma_1)$$

$$\cong \frac{R}{E} (\Delta\sigma_2 - \mu\Delta\sigma_1) , \qquad \text{(B-10)}$$

and the change in axial length of the element is

$$\delta x = \frac{dx}{E} (\Delta\sigma_1 - \mu\Delta\sigma_2) \quad . \qquad \text{(B-11)}$$

The volume enclosed by the newly stressed element is

$$\pi(R + \Delta R)^2(\delta x + dx), \qquad \text{(B-12)}$$

and the change in length of the original element BC compatible with this change in volume is

$$\frac{\pi(R + \Delta R)^2(\delta x + dx) - \pi R^2 dx}{\pi R^2} \quad . \qquad \text{(B-13)}$$

Neglecting terms that are very small compared to those retained, the total change in length of the element is

$$\delta x + \frac{2\Delta R}{R} dx \quad . \qquad \text{(B-14)}$$

From strength considerations, the total change in length of the element produced by a pressure change of wdH is

Figure 13. Differential pipe element

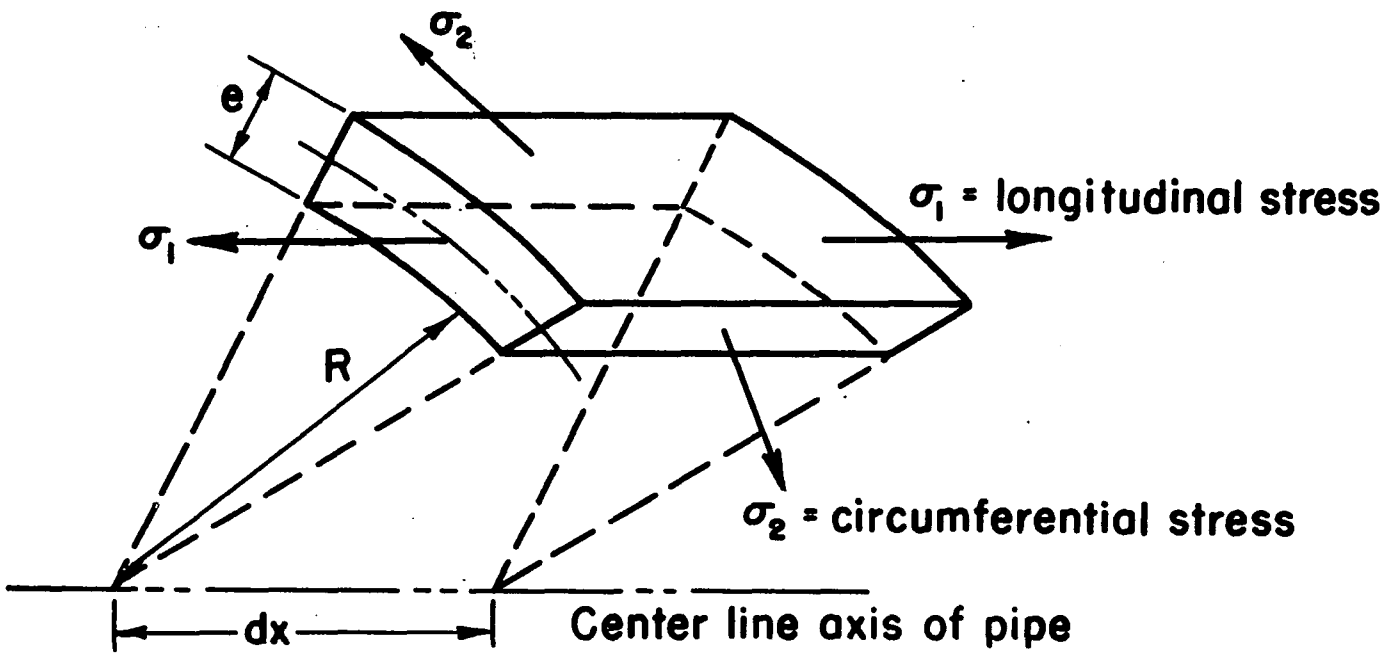
σ_2
e
σ_1
σ_1 = longitudinal stress
R
σ_2 = circumferential stress
dx
Center line axis of pipe

$$\frac{wDdH\ dx\ c}{E\ e} \quad , \tag{B-15}$$

where c depends upon the ability of the pipe to move in a longitudinal direction. Figure 14 gives values of c for different end constraints.

The change in volume of the original fluid element, dx in length, because of the elasticity of the fluid under the pressure change wdH, is

$$\frac{w\pi R^2}{K}\ dH\ dx \ , \tag{B-16}$$

and the corresponding change in length is

$$\frac{w\pi R^2}{K\pi R^2}\ dH\ dx = \frac{w}{K}\ dH\ dx \ . \tag{B-17}$$

The total change in length caused by wdH is then

$$w(\frac{1}{K} + \frac{Dc}{Ee})\ dH\ dx. \tag{B-18}$$

Since H is a function of x and t

$$dH = (\frac{\partial H}{\partial t} + V\frac{\partial H}{\partial x})dt \quad , \tag{B-19}$$

and recalling

$$\overline{BD} - \overline{CF} = -\frac{\partial V}{\partial x}\ dx\ dt = w(\frac{1}{K} + \frac{Dc}{Ee})\ dH\ dx, \tag{B-20}$$

then

$$-\frac{\partial V}{\partial x} = \frac{g}{a^2}(\frac{\partial H}{\partial t} + V\frac{\partial H}{\partial x}) \quad , \tag{B-21}$$

where

$$a = \sqrt{\frac{1}{\frac{w}{g}(\frac{1}{K} + \frac{Dc}{Ee})}} \quad . \tag{B-22}$$

Because it will be shown that "a" is the velocity of wave

Figure 14. Values of c for various end constraints on pipe

a)  $C = \frac{5}{4} - \mu$

b) 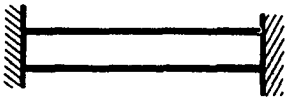 $C = 1 - \mu^2$

c)  $C = 1 - \frac{\mu}{2}$

propagation in the fluid

$$x = \pm at + \text{constant}, \tag{B-23}$$

therefore

$$dx = \pm adt , \tag{B-24}$$

and

$$V \frac{\partial V}{\partial x} = \frac{V}{a} \frac{\partial V}{\partial t} \tag{B-25}$$

$$V \frac{\partial H}{\partial x} = \frac{V}{a} \frac{\partial H}{\partial t} . \tag{B-26}$$

This means that if V/a is much less than one

$$V \frac{\partial V}{\partial x} \ll \frac{\partial V}{\partial t} , \tag{B-27}$$

and

$$V \frac{\partial H}{\partial x} \ll \frac{\partial H}{\partial t} , \tag{B-28}$$

and equations B-5 and B-21 reduce to

$$- \frac{\partial H}{\partial x} = \frac{1}{g} \frac{\partial V}{\partial t} + FV , \tag{B-29}$$

and

$$- \frac{\partial V}{\partial x} = \frac{g}{a^2} \frac{\partial H}{\partial t} . \tag{B-30}$$

If friction is neglected in B-29 and equations B-29 and B-30 are solved simultaneously, the classical wave equation results

$$\frac{\partial^2 H}{\partial t^2} = a^2 \frac{\partial^2 H}{\partial x^2} . \tag{B-31}$$

From previous solutions of this equation it was observed that "a" was the velocity of wave propagation.

APPENDIX C - DIGITAL COMPUTER PROGRAM FOR TAKING LAPLACE TRANSFORMS AND FINDING THE TRANSFER FUNCTION OF A SYSTEM

The Laplace transform of a function f(t) is defined as

$$\mathcal{L}\{f(t)\} = \int_0^\infty f(t)e^{-st}\,dt = F(s) \qquad \text{(C-1)}$$

If f(t) is known only from experimental curves and cannot easily be put into a mathematical form, the transform can be taken by numerical methods such as

$$F(s) = \sum_{n=0}^{\infty} \left\{ \frac{f[(n+1)\,\Delta t]\; e^{-(n+1)s\,\Delta t} + f(n\,\Delta t)e^{-ns\,\Delta t}}{2} \right\} \Delta t \qquad \text{(C-2)}$$

If $f(t) = 0$ for all $t > t_a$ then the summation need only be taken to $n = t_a/\Delta t$.

The form C-2 can be used in conjunction with a digital computer to find the Laplace transform of a function. If values of $f(n\Delta t)$ and Δt are placed in the computer, the summation C-2 can be computed for various values of s.

Because f(t) will remain finite in experimental work and the assumption will be made that $f(t) = 0$ for all t greater than some t_a, F(s) will remain finite for finite values of s. The assumption that $f(t) = 0$ for $t > t_a$, if not actually true, will cause more error for negative s, so it is better to confine s to positive values.

If the transform of an input $f_i(t)$ to a system with zero initial conditions is $F_i(s)$ and the transform of the output $f_o(t)$ is $F_o(s)$ the transfer function, $\overline{W}(s)$, of the system is defined as

$$\overline{W}(s) = \frac{F_o(s)}{F_i(s)} \qquad \text{(C-3)}$$

The computation of equation C-3 is easily implemented on a digital computer.

If more than one experimental run is made on a linear system the principle of superposition dictates that the average transfer function should be computed as

$$\overline{W}(s)_{ave.} = \frac{\sum_n F_o(s)_n}{\sum_n F_i(s)_n} \quad . \qquad \text{(C-4)}$$

Figure 15 is a flow diagram for a digital computer program to take experimental data from n runs on a linear system and calculate the transfer function for each run and also compute $\overline{W}(s)_{ave.}$ from equation C-4.

To compare experimental results with theory it is only necessary to compute the theoretical transfer function with the digital computer and compare this with the results from the preceding computation of $\overline{W}(s)_{ave.}$ from experimental data. Figure 16 is a flow diagram for a digital computer program to find the difference between experimental and analytical results and also to find the ratio of experimental to analytical results.

Table 4 is the results from the transfer function program given input and output data for a system having a transfer function

$$\overline{W}(s) = \frac{e^{-0.005s}}{s} \qquad \text{(C-5)}$$

Figure 15. Flow diagram for digital computer program to compute experimental transfer function

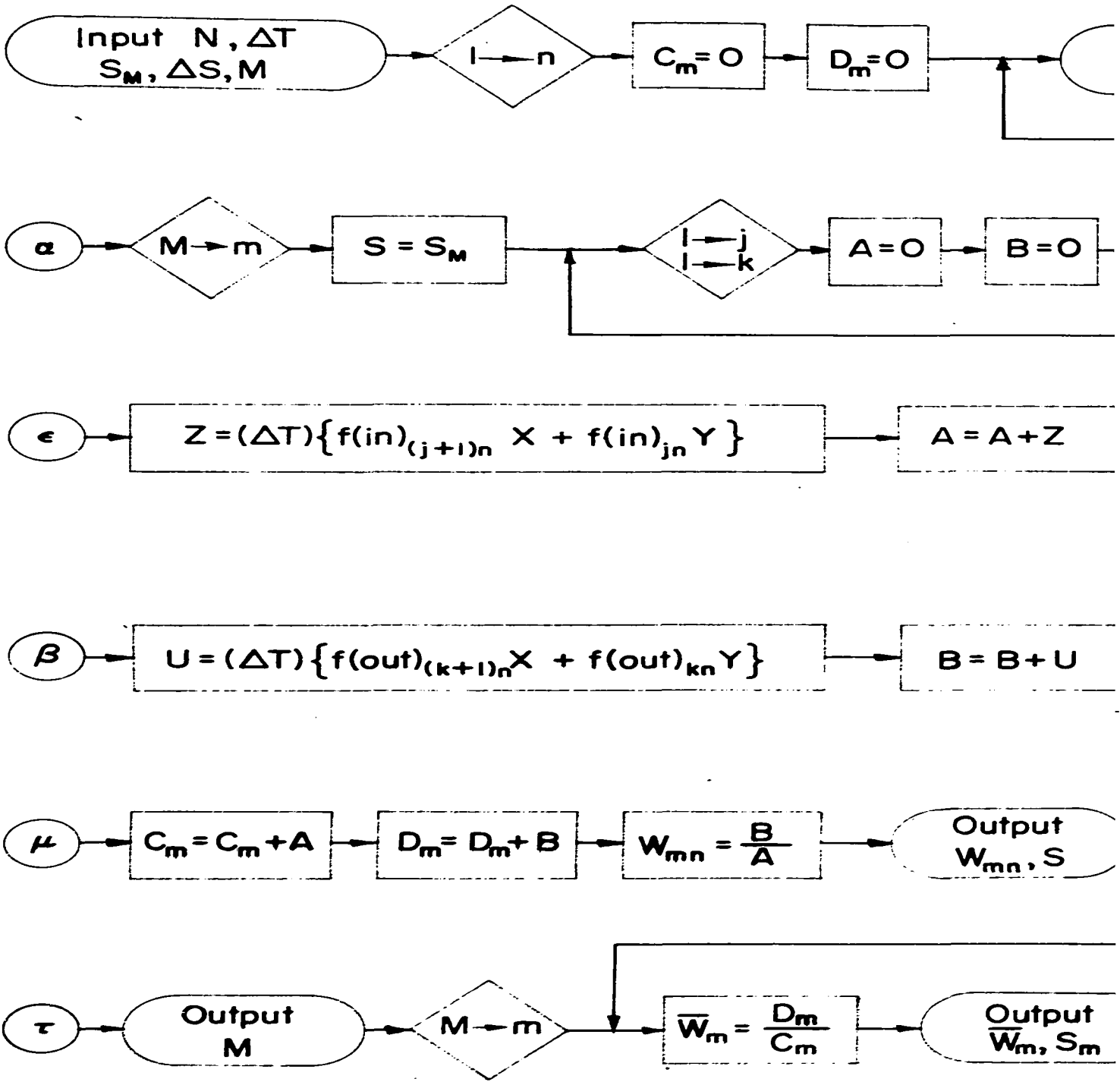
Input N, ΔT
S_M, ΔS, M
I → n
C_m = O
D_m = O
α
M → m
S = S_M
I → j
I → k
A = O
B = O
ε
Z = (ΔT){f(in)_(j+1)n X + f(in)_jn Y}
A = A + Z
β
U = (ΔT){f(out)_(k+1)n X + f(out)_kn Y}
B = B + U
μ
C_m = C_m + A
D_m = D_m + B
W_mn = B/A
Output
W_mn, S
τ
Output
M
M → m
W̄_m = D_m/C_m
Output
W̄_m, S_m

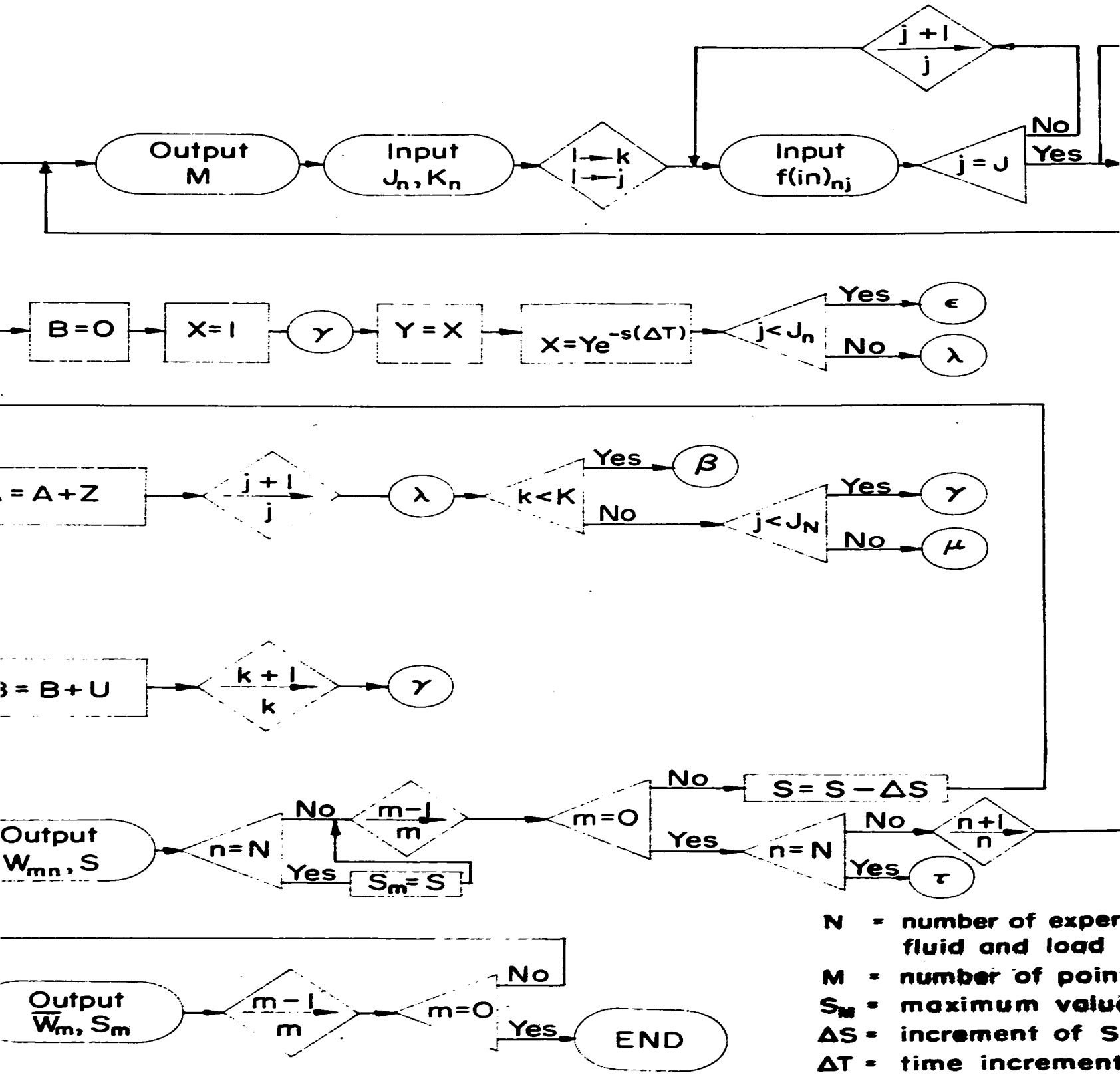

N = number of exper
fluid and load
M = number of poin
S_M = maximum valu
ΔS = increment of S
ΔT = time increment
J_n = number of data
K_n = number of data
W_{mn} = transfer functi
$\overline{W}_m$ = average transf

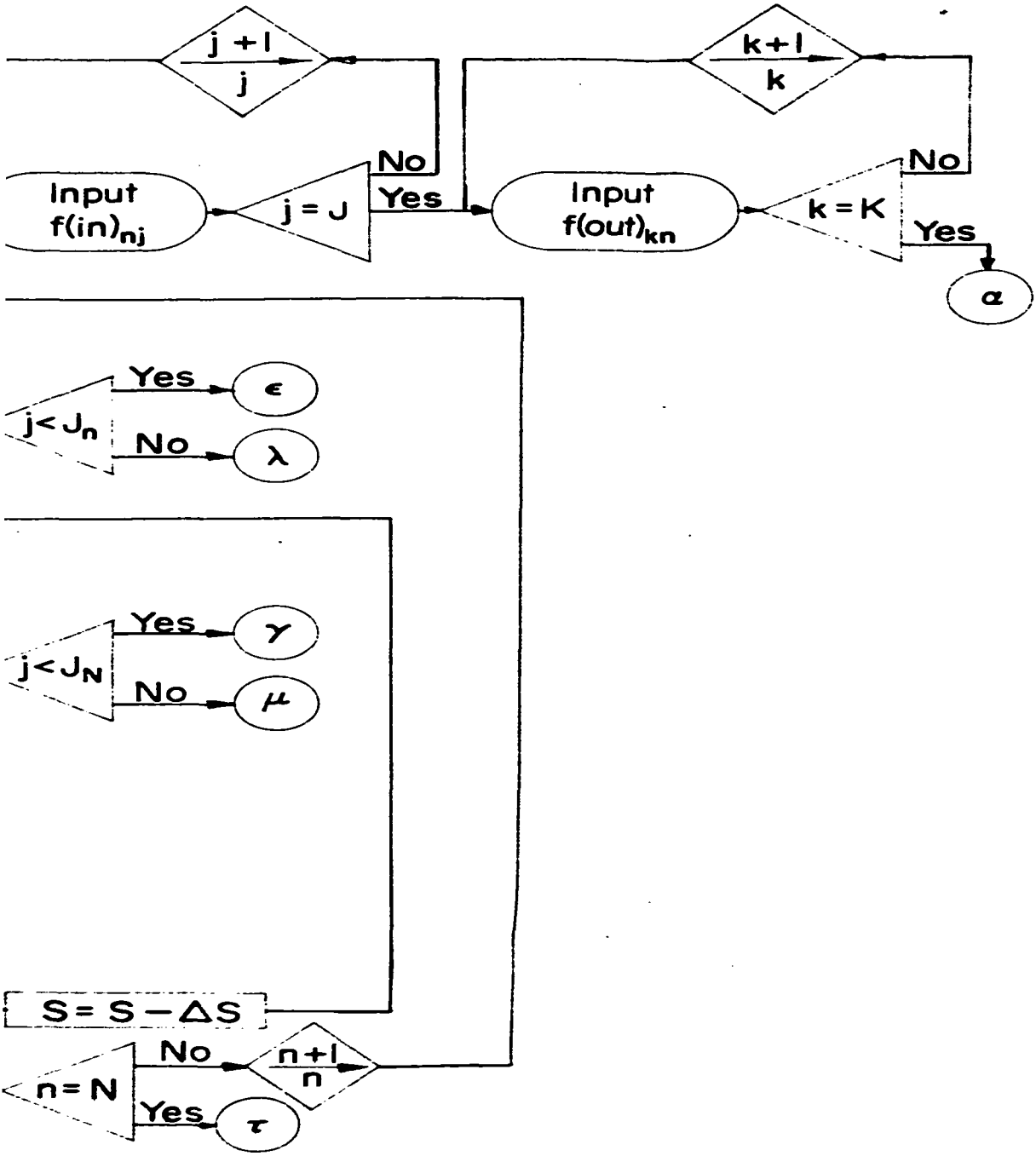

N = number of experimental runs for given fluid and load condition

M = number of points of S

S_M = maximum value of S

ΔS = increment of S

ΔT = time increment between experimental data pts.

J_n = number of data points of f(in) for run n

K_n = number of data points of f(out) for run n

W_{mn} = transfer function for run n

$\overline{W}_m$ = average transfer function for all N runs

Figure 16. Flow diagram for digital computer program to compare experimental to analytical transfer function

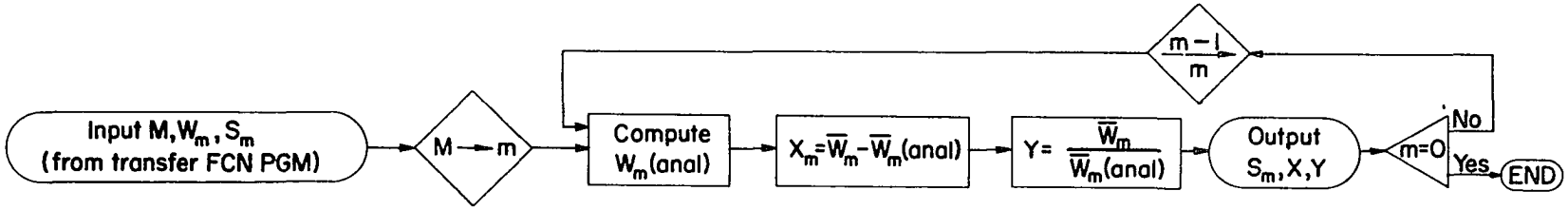

M = Number of points of S $\overline{W}_m$ = Average transfer function S_m = Values of S

$\overline{W}_m$(anal) = Transfer function computed from theoretical considerations

Table 4. Code check transfer function

s	$\overline{W}(s)_{exp} x 10^4$
20	452.38
40	204.62
60	123.39
80	83.70
100	60.55
120	45.62
140	35.35
160	27.96
180	22.46
200	18.27
220	15.00
240	12.43
260	10.36
280	8.69
300	7.33
320	6.20
340	5.27
360	4.49
380	3.84
400	3.29
420	2.83
440	2.43
460	2.10
480	1.82
500	1.58

and a one-cycle square-wave input

$$f_i(t) = u(t) - 2u(t-0.08)+u(t - 0.16) . \qquad (C-6)$$

The output then would be

$$f_o(t) =(t-0.005)u(t-0.005) -2(t-0.085)u(t-0.085)+ (t-0.165)u(t-0.165). \qquad (C-7)$$

Values of $f_i(t)$ and $f_o(t)$ were taken every 0.002 seconds.

Table 5 is the results from the computation to compare the experimental (that computed from equations C-6 and C-7) to the analytical (from equation C-5) transfer functions.

Table 5. Code check comparison of $\overline{W}_{exp}$ to $\overline{W}_{anal}$

s	$(\overline{W}_{anal}-\overline{W}_{exp})\times10^{6}$	$(\overline{W}_{exp}/\overline{W}_{anal})\times10^{2}$
20	3.01	99.99
40	5.46	99.97
60	7.41	99.94
80	8.93	99.89
100	10.09	99.83
120	10.96	99.76
140	11.56	99.67
160	11.95	99.57
180	12.15	99.46
200	12.21	99.33
220	12.14	99.19
240	11.97	99.04
260	11.72	98.88
280	11.40	98.71
300	11.04	98.52
320	10.64	98.31
340	10.21	98.10
360	9.77	97.87
380	9.32	97.63
400	8.86	97.38
420	8.40	97.12
440	7.95	96.84
460	7.50	96.56
480	7.07	96.26
500	6.65	95.95

APPENDIX D - ANALOG COMPUTER PROGRAM FOR SIMULATION OF A FLUID TRANSMISSION LINE

The simulation of equation 49 can be programmed on an analog computer as in Figure 17.

Because equation 49 was derived using the perturbation head, H, to find the total head it is necessary to introduce the steady-state pressure head, H_o. This effect can be simulated as in Figure 18. $\mathcal{H}(0,t)$ is the instantaneous input pressure head, and is divided by blocking capacitors into its steady-state and perturbation components. The perturbation component is passed through the circuit shown in Figure 17, while the steady-state component is modified by the factor

$$\frac{R_L}{R_p + R_L} \quad , \tag{D-1}$$

where R_L is the resistive component of the load impedance and R_p is the steady-state pipe resistance to flow. This relationship is based on the fact that in the steady-state the pipe and load act as a potential divider.

Figure 17. Analog computer diagram for simulation of equation 49

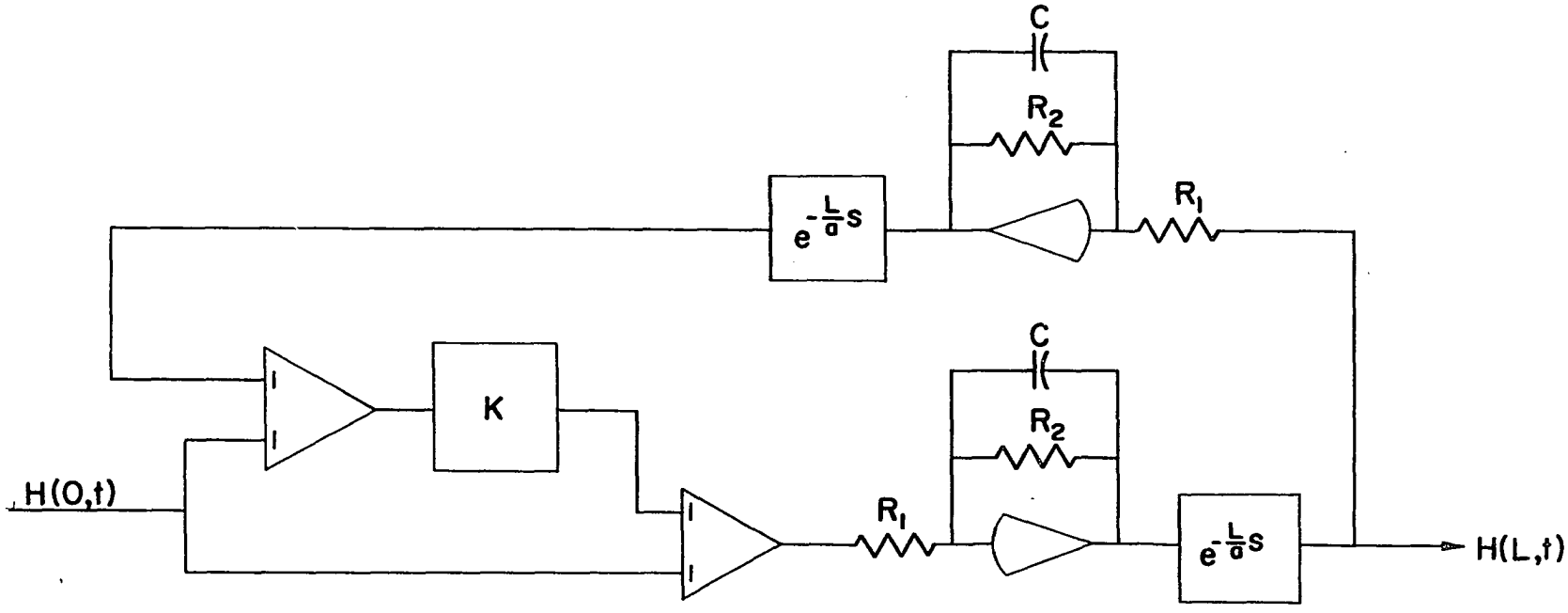

$e^{-\frac{L}{a}s}$ Dead time generator, $\frac{L}{a}$ seconds delay $\quad \frac{R_2}{R_1} = 1 \quad R_2C = \frac{1}{\omega_n} \quad k = \frac{Z_0 - Z_L}{Z_0 + Z_L}$

Figure 18. Analog computer diagram to obtain instantaneous output pressure

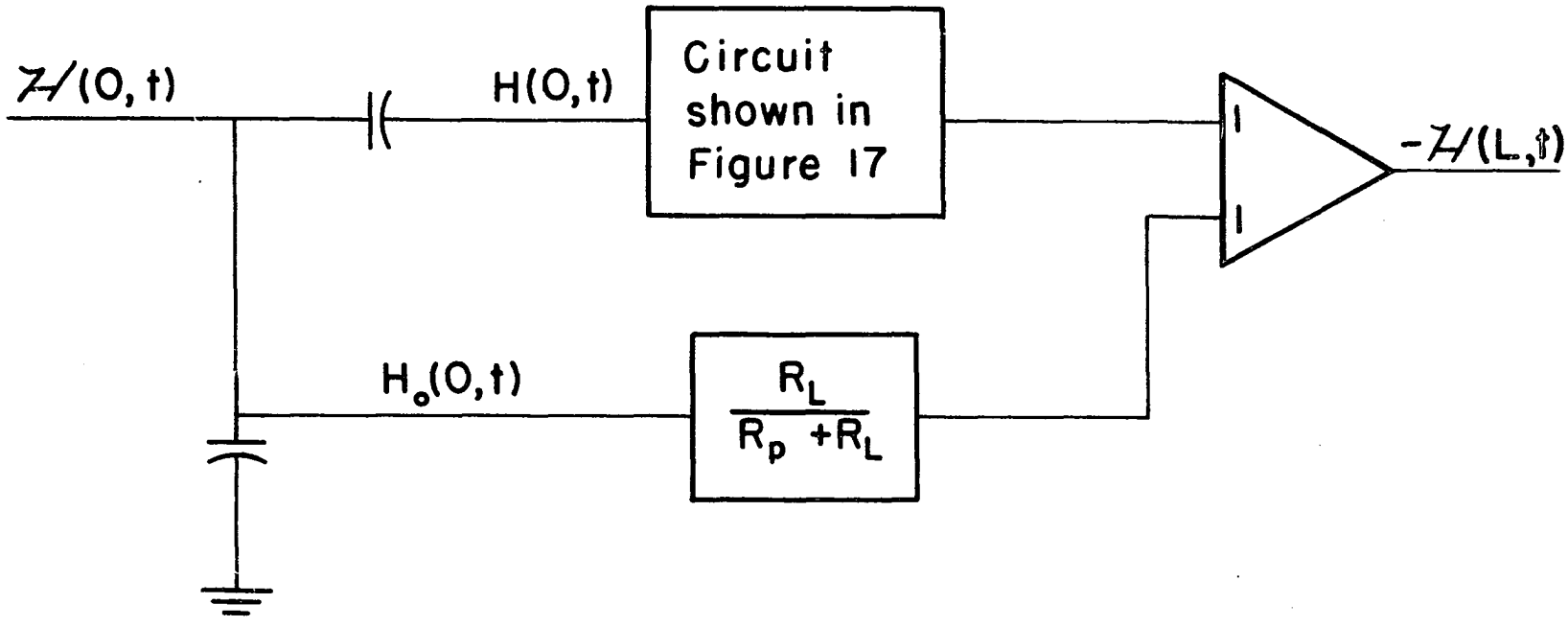
$\mathcal{H}(0,t)$
H(0,t)
Circuit shown in Figure 17
$-\mathcal{H}(L,t)$
$H_o(0,t)$
$\frac{R_L}{R_p + R_L}$

APPENDIX E - DERIVATION OF THE IMPEDANCE OF A TRAPPED-AIR FLUID CAPACITOR

Reference is made to Figure 19 which represents the fluid capacitor used in this investigation, and APPENDIX A - SYMBOLS AND NOTATION.

From continuity, and assuming incompressibility of the fluid

$$VA = A_c \frac{dy}{dt} . \qquad (E\text{-}1)$$

Noting that zero subscripts denote initial conditions, and assuming isentropic compression of the air,

$$Pv^n = P_o v_o^n , \qquad (E\text{-}2)$$

therefore

$$P = \frac{P_o v_o^n}{v^n} , \qquad (E\text{-}3)$$

where

$$v = v_o - yA_c . \qquad (E\text{-}4)$$

Using Newtonian notation for derivatives with respect to time,

from equation E-3 $$\dot{P} = \frac{-nP_o v_o^n}{v^{n+1}} (\dot{v}) , \qquad (E\text{-}5)$$

and from equation E-4

$$\dot{v} = -\dot{y}A_c , \qquad (E\text{-}6)$$

therefore, substituting equation E-6 into equation E-5 yields

$$\dot{P} = \frac{nP_o v_o^n A_c \dot{y}}{v^{n+1}} . \qquad (E\text{-}7)$$

If y is small, v approximately equals v_o, and equation E-7 becomes

$$\dot{P} = \frac{nP_oA_c\dot{y}}{v_o} \quad . \tag{E-8}$$

The pressure head H(L,t) is

$$H = y + h + \frac{P}{w} \quad , \tag{E-9}$$

therefore

$$\dot{H} = \dot{y} + \frac{\dot{P}}{w} \quad . \tag{E-10}$$

Substituting equation E-8 into equation E-10 gives

$$\dot{H} = \dot{y}(1 + \frac{nP_oA_c}{wv_o}) \, . \tag{E-11}$$

Solving 1 for $\dot{y}$ and substituting into equation E-11 gives

$$\dot{H} = \frac{VA}{A_c}(1 + \frac{nP_oA_c}{wv_o}) \, . \tag{E-12}$$

Now

$$v_o = l_oA_c \quad , \tag{E-13}$$

therefore equation E-12 becomes

$$\dot{H} = \frac{VA}{A_c}(1 + \frac{nP_o}{wl_o}) \quad . \tag{E-14}$$

Taking the Laplace transform of equation E-14 and dividing both sides by the transform of V(L,t) gives, by definition, the load impedance which is

$$Z_L = \frac{1}{s}\frac{A}{A_c}(1 + \frac{nP_o}{wl_o}) \quad , \tag{E-15}$$

or

$$Z_L = \frac{1}{s}(\frac{D}{d})^2 (1 + \frac{nP_o}{wl_o}) \quad . \tag{E-16}$$

Therefore

$$Z_L = \frac{C}{s} , \tag{E-17}$$

the impedance of a capacitive element.

As an example, for series number 2, Table 1,

$$Z_L = \frac{1}{s} \left(\frac{2.073}{0.312}\right)^2 \left(1 + \frac{(1.4)(17.2)(1728)}{(49.3)(2.25)}\right. \tag{E-18}$$

$$= 16,500/s . \tag{E-19}$$

Figure 19. Trapped-air fluid capacitor

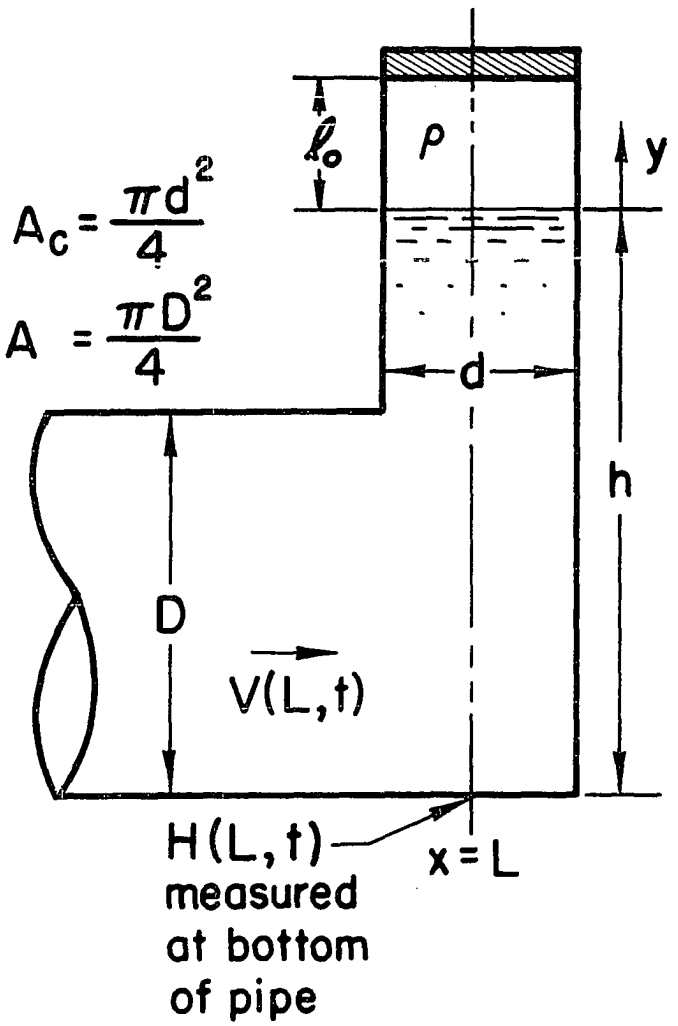
$A_c = \frac{\pi d^2}{4}$
$A = \frac{\pi D^2}{4}$
ℓ_o
ρ
y
d
h
D
$\vec{V}(L,t)$
H(L,t)
measured
at bottom
of pipe
x = L